

The role of anaerobic respiration in the immobilization of uranium through biomineralization of phosphate minerals

Kathleen R. Salome ^a, Stefan J. Green ^{b,f}, Melanie J. Beazley ^{a,c}, Samuel M.
Webb ^d, Joel E. Kostka ^{a,e}, Martial Taillefert ^a

^a School of Earth and Atmospheric Sciences, Georgia Institute of Technology, Atlanta, GA 30332-0340, ^b DNA Services Facility, Research Resource Center, University of Illinois at Chicago, Chicago, IL, ^c Present address: Department of Biological Sciences, University of Alabama, Tuscaloosa, AL, ^d Stanford Synchrotron Radiation Lightsource, Menlo Park, CA 94025, ^e School of Biology, Georgia Institute of Technology, Atlanta, GA 30332-0340, ^f Department of Biological Sciences, University of Illinois at Chicago, Chicago, IL

Revised for *Geochimica et Cosmochimica Acta*

11/28/2012

1 **ABSTRACT**

2 Although bioreduction of uranyl ions (U(VI)) and biomineralization of U(VI)-phosphate
3 minerals are both able to immobilize uranium in contaminated sediments, the competition
4 between these processes and the role of anaerobic respiration in the biomineralization of
5 U(VI)-phosphate minerals has yet to be investigated. In this study, contaminated
6 sediments incubated anaerobically in static microcosms at pH 5.5 and 7.0 were amended
7 with the organophosphate glycerol-2-phosphate (G2P) as sole phosphorus and external
8 carbon source and iron oxides, sulfate, or nitrate as terminal electron acceptors to
9 determine the most favorable geochemical conditions to these two processes. While
10 sulfate reduction was not observed even in the presence of G2P at both pHs, iron
11 reduction was more significant at circumneutral pH irrespective of the addition of G2P.
12 In turn, nitrate reduction was stimulated by G2P at both pH 5.5 and 7.0, suggesting
13 nitrate-reducing bacteria provided the main source of inorganic phosphate in these
14 sediments. U(VI) was rapidly removed from solution in all treatments but was not
15 reduced as determined by X-ray absorption near edge structure (XANES) spectroscopy.
16 Simultaneously, wet chemical extractions and extended X-ray absorption fine structure
17 (EXAFS) spectroscopy of these sediments indicated the presence of U-P species in
18 reactors amended with G2P at both pHs. The rapid removal of dissolved U(VI), the
19 simultaneous production of inorganic phosphate, and the existence of U-P species in the
20 solid phase indicate that uranium was precipitated as U(VI)-phosphate minerals in
21 sediments amended with G2P. Thus, under reducing conditions and in the presence of
22 G2P, bioreduction of U(VI) was outcompeted by the biomineralization of U(VI)-
23 phosphate minerals and U(VI) sorption at both pHs.

1. INTRODUCTION

The United States Department of Energy (DOE) currently manages 120 nuclear legacy waste sites spread over 36 states contaminated with heavy metals and radionuclides, such as uranium (U) (DOE, 1997; NABIR, 2003). As the sheer volume of contaminated geomedia at these sites makes traditional remediation techniques (i.e. pump-and-treat, excavation) cost-prohibitive (Dawson and Gilman, 2001; Jardine, 2006; Mackay and Cherry, 1989), remedial efforts have focused on the development of alternative *in situ* technologies designed to immobilize contaminants in the subsurface.

As with other contaminants, the design of uranium *in situ* remediation techniques aims to capitalize on the geochemical properties of uranium in natural waters to immobilize it in the subsurface. Uranium mobility in groundwater is largely driven by ligand complexation (i.e. carbonate), adsorption to metal oxides, and precipitation reactions (i.e. formation of phosphate minerals, reduced metal oxides). In oxic groundwater where U(VI) is the dominant oxidation state, uranium usually occurs as the highly mobile uranyl ion UO_2^{2+} (Langmuir, 1997). The dominant aqueous forms of uranyl in the environment include the free uranyl ion at low pH and positively charged hydroxyl complexes at circumneutral pH ($5 \leq \text{pH} \leq 6.5$) (Langmuir, 1997). At pH 5.0, aqueous U(VI) adsorbs strongly to manganese oxides given their low pH_{zpc} (Han et al., 2007) and even to ferric oxides despite the net positive charge of both uranyl hydroxide complexes and metal oxides (Han et al., 2007; Hsi and Langmuir, 1985; Waite et al., 1994). Ferric oxides represent one of the most important U(VI) sorbents in soils of the Oak Ridge Field Research Center (ORFRC), a well-studied nuclear legacy waste site in Oak Ridge, TN, and at pH 5.5 and 7.0 approximately 80% and 98% of U(VI) adsorbs to

1 these soils (Barnett et al., 2002). In addition, the presence of inorganic phosphate may
2 enhance U(VI) sorption to ferric oxides at low pH through the formation of ternary
3 surface complexes (Cheng et al., 2004; Payne et al., 1996). In higher pH environments
4 ($\text{pH} \geq 7.0$) and in the presence of elevated concentrations of carbonates, uranyl carbonate
5 complexes represent the dominant form of U(VI) in solution (Langmuir, 1997). These
6 complexes only minimally adsorb to iron oxides (Katsoyiannis, 2007), and the presence
7 of elevated carbonate promotes both U(IV) and U(VI) mineral dissolution (De Pablo et
8 al., 1999; Liu et al., 2004; Sowder et al., 2001; Ulrich et al., 2009). In addition, elevated
9 calcium concentrations present in high pH environments may promote the formation of
10 ternary calcium-uranyl-carbonate complexes, which further inhibit U(VI) sorption (Fox et
11 al., 2006; Meleshyn et al., 2009; Stewart et al., 2010) and U(VI) reduction by lowering
12 the reduction potential of uranium to less energetically favorable values (Brooks et al.,
13 2003; Luo et al., 2007). Therefore, uranium mobility in circumneutral pH environments
14 may be largely driven by carbonate dissolution and complexation reactions.

15 In reducing environments, uranium is either chemically or biologically reduced to
16 insoluble U(IV) minerals, including uraninite (Finch and Murakami, 1999; Langmuir,
17 1997) or non-uraninite minerals (Bernier-Latmani et al., 2010; Fletcher et al., 2010;
18 Sharp et al., 2011). At $\text{pH} > 6$, the surface-catalyzed chemical U(VI) reduction by Fe(II)
19 adsorbed onto crystalline iron oxides (Behrends and Van Cappellen, 2005; Jeon et al.,
20 2005; Liger et al., 1999; Regenspurg et al., 2009) and other minerals (Chakraborty et al.,
21 2010; Regenspurg et al., 2009) may also occur. Dissolved sulfide (Ho and Miller, 1986;
22 Kosztolanyi et al., 1996; Mohagheghi et al., 1985) and sulfide minerals (Beyenal et al.,
23 2004; Marsili et al., 2007; Wersin et al., 1994) have also been shown to reduce U(VI)

1 chemically. In addition, several strains of metal-reducing and sulfate-reducing bacteria
2 are capable of reducing U(VI) (reviewed in Kostka and Green, 2011), including members
3 of the genus *Shewanella* (Blakeney et al., 2000; Lovley et al., 1991), *Desulfovibrio* sp.
4 (Lovley and Phillips, 1992), *Geobacter* sp. (Jeon et al., 2004; Lovley et al., 1991), and
5 *Anaeromyxobacter dehalogens* (Sanford et al., 2007). Biologically-mediated reduction of
6 U(VI), or bioreduction, is currently the primary *in situ* remediation technique studied for
7 the immobilization of uranium in subsurface environments (Fredrickson et al., 2000;
8 Ganesh et al., 1999; Lovley and Phillips, 1992; Lovley et al., 1991; North et al., 2004;
9 Sanford et al., 2007; Wade and DiChristina, 2000), and *in situ* bioreduction of U(VI) has
10 been demonstrated at the ORFRC (Wu et al., 2006b) and other contaminated sites (Senko
11 et al., 2002). Unfortunately, bioreduction is inhibited at $\text{pH} < 7$ and in elevated nitrate
12 concentrations (Finneran et al., 2002b; Wu et al., 2006a; Wu et al., 2006b). In addition,
13 the uraninite mineral product may not remain stable in fluctuating chemical conditions as
14 uraninite is readily oxidized to the mobile U(VI) upon reintroduction of oxygen in
15 groundwater recharge areas (Langmuir, 1997; Murphy and Shock, 1999) and by NO_2^-
16 (Beller, 2005; Moon et al., 2007; Wu et al., 2010), $\text{Fe}(\text{OH})_3$ (Senko et al., 2002; Senko et
17 al., 2005b; Wan et al., 2005), and MnO_2 (Fredrickson et al., 2002) under reducing
18 conditions. Thus, the long term instability of uraninite coupled with the inhibitory effects
19 of co-contaminants on U(VI) reduction favors investigation of alternative remediation
20 techniques applicable in both reducing and oxidizing conditions.

21 Biomineralization of insoluble U(VI)-phosphate minerals through the activities of
22 microbial phosphatases represents a possible complementary bioremediation technique to
23 bioreduction. U(VI) forms sparingly soluble and stable (Jerden and Sinha, 2003)

1 phosphate minerals over a broad range of environmental conditions (pH 4 - 8) (Ohnuki et
2 al., 2004; Wellman et al., 2007; Zheng et al., 2006), and uranium phosphate minerals
3 have been identified in sediments from the ORFRC (Kelly et al., 2005; Roh et al., 2000;
4 Stubbs et al., 2006) and the Hanford 300 Area facility, WA (Arai et al., 2007; Catalano et
5 al., 2006), among others. As inorganic phosphate readily adsorbs to soils ($\text{pH} \leq \sim 7.0$) or
6 precipitates as minerals ($\text{pH} \geq \sim 4.0$) ultimately decreasing the hydraulic conductivity of
7 soils (Wellman et al., 2006), direct addition of inorganic phosphate to subsurface
8 environments is not a viable field-scale remediation strategy. Thus, research has focused
9 primarily on stimulating microbially-mediated phosphate production coupled to a
10 chemical precipitation of sparingly soluble U(VI)-phosphate minerals (Beazley et al.,
11 2007, 2009; Macaskie et al., 1995; Martinez et al., 2007; Montgomery et al., 1995;
12 Shelobolina et al., 2009). To fulfill their phosphate requirements, most microorganisms
13 produce phosphatase enzymes, a class of non-specific enzymes that catalyze the
14 hydrolysis of organic phosphoester bonds in a broad range of chemical conditions
15 (Rossolini et al., 1998). Uranium removal coupled to phosphatase activity has been
16 demonstrated in both aerobic and anaerobic conditions and at both acidic and
17 circumneutral pH by the facultative anaerobe *Rahnella* sp. Y9602 (Beazley et al., 2007,
18 2009; Martinez et al., 2007) and in low-pH aerobic conditions by *Citrobacter* sp.
19 (Macaskie et al., 1995; Montgomery et al., 1995). In addition, uranium removal in
20 aerobically-maintained contaminated sediments has been achieved through stimulation of
21 the phosphatase activities of indigenous bacteria (Beazley et al., 2011; Shelobolina et al.,
22 2009). As phosphatases may also be activated in anaerobic conditions (Rossolini et al.,
23 1998), U(VI)-phosphate biomineralization may compete with bioreduction in the

1 presence of G2P. Interestingly, the competitive interaction between these two processes
2 has yet to be investigated.

3 In this study, a combination of X-ray absorption spectroscopy, solid-phase
4 extractions, and bulk chemical analyses was used to determine whether nitrate-, iron-, or
5 sulfate-reducing conditions are most conducive to uranium removal through the activity
6 of endogenous microbial phosphatases in contaminated sediments from the ORFRC. In
7 addition, the competition between uranium reduction and the biomineralization of U(VI)-
8 phosphate minerals under varying electron accepting conditions in both low and
9 circumneutral pH environments was examined.

10 **2. EXPERIMENTAL**

11 **2.1 Materials and Site Description**

12 Contaminated sediments were collected during installation of a monitoring well in
13 Area 3 of the ORFRC (well number: FWB120-08-40, core depth: 21-23'; courtesy of D.
14 Watson, ORNL). Soil mineralogy of neighboring wells indicates a bulk soil particle size
15 distribution (~1.5 m depth) as 31% sand, 50% silt, and 19% clay (Barnett et al., 2000). In
16 addition, bulk soil Mn and Fe content in Oak Ridge have been quantified as 0.36 g/kg and
17 25.8 g/kg, respectively (Barnett et al., 2000), and uranium-bearing Fe and Mn minerals in
18 Area 3 Oak ridge soils have been identified as polycrystalline ferrihydrite and goethite
19 and poorly crystalline mixed Mn-Fe oxides (Stubbs et al., 2006). As Area 3 sediments
20 are located closest to the former waste disposal ponds, they are generally characterized by
21 low pH and high nitrate levels (Brooks, 2001). Chemical information for well FWB120
22 remains unavailable; however, the nearest neighboring well (~1 m) displays an average
23 pH of 3.4, nitrate concentration of 30.4 mM, and sulfate concentration of 19.7 mM.

Sediment cores were stored in the dark at 4°C and remained sealed until incubation.

2.2 Experimental Design

To simulate a variety of environmental conditions, static microcosms containing 125 g of contaminated ORFRC sediments homogenized under controlled atmosphere (1% H₂, 5% CO₂, 94% N₂) were incubated in duplicate in 1-L borosilicate glass reactors containing sterile artificial groundwater for a period of 70 days. In each treatment, 500 mL of artificial groundwater containing 17.1 mM NaCl, 2.0 mM MgCl₂•6H₂O, 680 µM CaCl₂•2H₂O, and 6.7 mM KCl was first degassed using UHP N₂, sealed, and autoclaved. After cooling, filter-sterilized aliquots of selenite-tungstate solution (0.1%), trace elements solution (0.1%, Table S1, (Bak, 1992)), NaHCO₃ (5 mM), and either 2-(N-Morpholino)ethanesulfonic acid (MES, 50 mM, pH 5.5) or 4-(2-hydroxyethyl)-1-piperazineethanesulfonic acid (HEPES, 50 mM, pH 7.0) were added to autoclaved groundwater in the presence or absence of filter-sterilized solutions of glycerol-2-phosphate (G2P) (Sigma Aldrich) and uranyl acetate (Spectrum) (Table 1). Reactors were buffered at pH 5.5 or 7.0 to establish conditions favorable to both U(VI)-phosphate biomineralization (pH 5.5) and bioreduction (pH 7.0). Excluding G2P, no external electron donor was added to the system. Reactors were sealed from the controlled atmosphere within an hour after addition of the reactants, such that the incubations were not significantly affected by H₂ and CO₂ gases. Sealed duplicate reactors were homogenized to ensure uniform groundwater composition prior to static incubation at room temperature in the dark.

At each time point, the following sampling protocol was followed to ensure that all samples were maintained anaerobic at all times. Microcosm sediment and

groundwater were homogenized, and a subsample of the microcosm mixture was extracted under anaerobic atmosphere (1% H₂, 5% CO₂, and 94% N₂) through a septum using a polypropylene syringe with Teflon plunger (HSW) and a 18 gauge stainless steel needle (B & H). An aliquot of the homogenized mixture was added to a 0.5 M HCl solution to extract total Fe(II). The remaining mixture was centrifuged at 3300 rpm for 5 minutes. The supernatant was filtered through a 0.2 µm pore size polyethersulfane membrane filter (Puradisc, Whatman) and reserved for pH measurement (data not shown) and analysis of phosphate and nitrite. Other filtered aliquots were diluted in 2% trace metal grade nitric acid for uranium analysis or preserved in 0.1 M HCl and stored at 4°C until dissolved Fe(II) quantification. The remaining filtered supernatant was frozen until analysis of sulfate, nitrate, and G2P. Finally, following completion of the incubations, sediments were collected for solid-phase chemical extraction, X-ray absorption near-edge spectroscopy (XANES), and extended X-ray absorption fine structure (EXAFS) analysis. Sediments were preserved at -80°C and under UHP N₂ atmosphere in Mason jars until analysis.

2.3 Analytical Methods

2.3.1 Aqueous Phase Speciation

Dissolved uranium was measured in duplicate using an Agilent 7500a Series inductively coupled plasma mass spectrometer (ICP-MS). Standards were prepared using uranyl acetate (Spectrum) acidified in 2% trace metal grade nitric acid (Fisher). Holmium and bismuth were used as internal references in both standards and samples (SPEX certiPrep), and 2% trace metal grade nitric acid blanks and calibration check standards were used as quality controls. Phosphate, nitrite, and total/dissolved Fe(II) were

quantified colorimetrically with a Milton Roy Spectronic 501 spectrophotometer. Phosphate was measured using the molybdenum blue method (Murphy and Riley, 1962), nitrite was measured using a sulphanilamide/NED reagent mixture immediately after sampling (Grasshoff, 1983), and Fe(II) was measured using the ferrozine method (Stookey, 1970). Adsorbed Fe(II) was quantified by difference of total Fe(II), measured in unfiltered acidified samples, and dissolved Fe(II) determined in filtered samples. Sulfate, nitrate, and G2P were measured by ion chromatography using a Dionex GP-50 HPLC pump and conductivity detector (Dionex, CD-20) coupled to an Analytical Instrument Systems, Inc. integrator (LCC 100). An anion exchange analytical column (Dionex AS14, 4 x 250mm) and guard column (Dionex AG14, 4 x 50mm) were used in line with an AMMS-300 (4-mm, Dionex) suppressor. Operating conditions included a 10% acetonitrile, 1 mM NaHCO₃, and 3 mM Na₂CO₃ buffer eluent with a 1 mL min⁻¹ flow rate and a 25 mN H₂SO₄ regenerant. All standard deviations reported for dissolved species represent the range of average concentrations found in duplicate reactors.

2.3.2 Rate Constant Calculations and Thermodynamic Modeling

Rate constants, k_{obs} , for NO₃⁻ consumption, G2P consumption, and U removal were calculated assuming pseudo-first-order reactions using the linear regression of the natural log of concentrations as a function of time (see details in supplementary information). The error reported for rate constants was propagated to include variations between duplicate incubations and standard error of the unweighted slope of linear regressions. Due to the apparent two-phased uranium removal, two separate uranium rate constants were calculated for pH 5.5 reactors; U_0 represents the rate constant calculated for days 0 – 4 and U_7 represents the rate constant calculated for days 7 – 31.

Thermodynamic equilibrium calculations were performed in MINEQL+ (Schecher and McAvoy, 2001) for each reactor treatment. The theoretical composition of artificial groundwater, modified to reflect the different treatments (Table 1), was included as the background solution in the thermodynamic calculations. For these calculations, total ΣPO_4^{3-} concentrations in all G2P-containing reactors were estimated assuming complete hydrolysis of the organophosphate compound, and total Fe(II) detected at 7 days was used to estimate the maximum Fe(II) production. Adsorption onto amorphous iron oxides was included using a double-layer sorption model with both low affinity and strong affinity sites and solid concentrations that reflected the composition of ORFRC soils (Barnett et al., 2002). Ionic strength was calculated, and the system was assumed to be closed to the atmosphere with a pH of 5.5 or 7.0 and total dissolved inorganic carbon concentrations fixed at 5 mM.

2.3.3 Solid phase uranium characterization

Solid phase uranium and phosphate eventually associated with the solid phase were quantified in duplicates in sediments collected following 70 days of incubation using a modified sequential extraction technique of Tessier et al. (1979). The following procedure was performed sequentially: (1) 4 mL of 1.0 M MgCl_2 (pH 7.0) was added to ~ 0.5 g sediment and agitated at 20°C for 1 hour to extract loosely adsorbed uranium; (2) 4 mL of 1.0 M sodium acetate (adjusted to pH 5.0 with 1.0 M HCl) was added and agitated at 20°C for 5 hours to dissolve uranium-phosphate minerals (Beazley et al., 2011); (3) 10 mL of 0.04 M $\text{NH}_2\text{OH} \cdot \text{HCl}$ in 25% (v/v) acetic acid was added and agitated at 96°C for 6 hours to remove Fe- and Mn-associated uranium; (4) 1.5 mL of 0.02 M HNO_3 and 2.5 mL of 30% H_2O_2 (pH 2.0) were added and agitated at 96°C for 2

1 hours, a second 1.5 mL aliquot of 30% H_2O_2 (pH 2.0) was added and agitated at 96°C for
2 3 hours, and a third 5 mL aliquot of 2.5 M NH_4OAc in 20% (v/v) HNO_3 was added and
3 agitated at 20°C for 1 hour to extract uranium bound to organics; and (5) 5 mL of 15.8 M
4 HNO_3 was added and maintained at 85°C for 3 hours to extract the residual fractions
5 (Gleyzes et al., 2002). After each extraction step, samples were centrifuged (1380 xG for
6 10 minutes), and supernatants were filtered (0.2 μm , PES Puradisc Whatman) and
7 reserved for uranium analysis by ICP-MS and for phosphate quantification using the
8 spectrophotometric technique of Murphy and Riley (1962). The pH of the samples for
9 phosphate quantification in each extract was adjusted to ~ 4.0 with NaOH (10.0 M) or
10 HCl (12.0 M) to allow for color development. Standards were prepared in extraction
11 media and treated as described above.

12 X-ray absorption spectroscopy (XAS) was performed at the Stanford Synchrotron
13 Radiation Lightsource (SSRL). Final samples (T = 70 days) from the U-amended
14 controls, the G2P-amended reactors, nitrate-amended reactors, and the sulfate-amended
15 reactors at both pH 5.5 and 7.0 were characterized by XAS, and an initial sample (T = 0
16 days) from pH 5.5 G2P-amended reactors was also examined. Sediment samples were
17 loaded into windowed Lexan sample holders, sealed with Kapton tape in an anaerobic
18 chamber (Coy Laboratory Instruments, Inc.), and maintained anoxic in a sealed jar for
19 transport to SSRL and under N_2 atmosphere at the beam line. Uranium L_{III} -edge XAS
20 spectra were collected at SSRL beam line 10-2 using a focused X-ray beam with a 23
21 keV harmonic rejection cutoff and a 13 element Ge detector. The incident energy was
22 selected with a Si(220) monochromator crystal. Transmission and fluorescence data were
23 collected simultaneously. Detection limits of around 5% weight are achieved in these

conditions at beam line 10-2. All EXAFS data were reduced using SIXPACK (Webb, 2005). Phase and amplitude files for EXAFS fittings were created with FEFF7 (Ankudinov et al., 1998; Zabinsky et al., 1995). Theoretical models were based on scattering paths expected for autunite-type group minerals (Catalano and Brown, 2004) and U(VI) adsorbed to iron oxihydroxides (Waite et al., 1994). The models were first tested on known chernikovite and U-Fe_(ads) samples to ensure good agreement with previous fittings (Beazley et al., 2009, 2011). The U=Oax=U=Oax transoxido multiple scattering path (Allen et al., 1996; Bargar et al., 2000; Hudson et al., 1996) was included in all fits. The axial oxygen coordination number (N) for all reactors was set at two (Beazley et al., 2007, 2009; Beazley et al., 2011; Webb et al., 2006). To aid comparison between samples, the Debye-Waller factors (σ) were fixed for shells other than axial oxygen, a common practice for uranium EXAFS (Bargar et al., 2000; Beazley et al., 2009; Beazley et al., 2011; Webb et al., 2006). The addition of shells was considered to improve the quality of the EXAFS fit if a reduction in the reduced chi-square was observed (Webb et al., 2006; Webb et al., 2005).

3. RESULTS

3.1 Aqueous species

The pH remained constant for the duration of the experiments in both pH 5.5 and 7.0 reactors (data not shown). In all treatments without addition of external terminal electron acceptors (TEAs), background nitrate and sulfate concentrations exchanged from the original sediment after 3 hours of equilibration averaged 450 μ M and 800 μ M, irrespective of the pH of the incubations (Figure 1A-D). Although sulfate and nitrate were present in the U-amended controls, both nitrate and sulfate reduction were

negligible without G2P addition (Figure 1A-D), even in pH 7.0 incubations in the presence of 7 mM NO_3^- (Figure 1D). After a phase lag of 15 days, the presence of G2P stimulated nitrate reduction at both pH 5.5 and 7.0 (Figure 1E-H) but not sulfate reduction, even in treatments containing elevated sulfate concentrations (Figure 1A-B), and complete depletion of nitrate was observed in G2P-containing reactors without NO_3^- addition after 39 days of incubation (Figure 1C-D). Pseudo-first-order rate constants for nitrate reduction in G2P-containing reactors unamended with nitrate were calculated to be $0.04 \pm 0.01 \text{ d}^{-1}$ and $0.07 \pm 0.03 \text{ d}^{-1}$ at pH 5.5 and 7.0 (Table 2). Although nitrate was removed in the sulfate-amended reactors, only ephemeral accumulation of nitrite was observed, while traces of nitrite were observed in the G2P-amended reactors with no external TEA (Figure 1C-D). In the nitrate-amended reactors at pH 5.5, nitrate concentrations were reduced from 7 to 2 mM over 70 days (Figure 1C) with a pseudo-first-order rate constant of $0.02 \pm 0.00 \text{ d}^{-1}$ (Table 2), and the accumulation of 4 mM nitrite was observed after a small phase lag (Figure 1C).

Aqueous Fe(II) remained constant at $\sim 10 \text{ }\mu\text{M}$ in both pH 5.5 and pH 7.0 reactors throughout the 21 day sampling period (Figure 1E-F). In all pH 5.5 reactors, adsorbed Fe(II) remained constant at $15 \text{ }\mu\text{M}$ until day 7 when a steep increase to $100 \text{ }\mu\text{M}$ was observed (Figure 1E). A much more pronounced increase in adsorbed Fe(II) was detected in all pH 7.0 reactors, irrespective of the TEA present, with concentrations as high as 1.1 mM (Figure 1F). A pseudo-first-order rate constant for Fe(III) reduction of $0.61 \pm 0.05 \text{ d}^{-1}$ was calculated from total Fe(II) produced at pH 5.5, while an average pseudo-first-order rate constant of $1.34 \pm 0.04 \text{ d}^{-1}$ was estimated for all treatments at pH 7.0 (Table 2). The increase in adsorbed Fe(II) was followed by a steady decrease to $\sim 65 \text{ }\mu\text{M}$ after 21 days

1 of incubation in all reactors at both pH (Figure 1E-F). The same trends were observed in
2 all reactors, regardless of the presence or absence of G2P.

3 Although G2P-containing reactors were amended with 5 mM G2P, initial aqueous
4 G2P concentrations averaged only 1 mM at pH 5.5 and 2.3 mM at pH 7.0 (Figure 1G-H),
5 indicating adsorption of G2P onto ORFRC sediments is more significant at low pH.
6 Complete removal of dissolved G2P was observed after 39 days of incubation (Figure
7 1G-H), and the pseudo-first-order rate constant for G2P consumption at pH 5.5 and 7.0
8 averaged $0.05 \pm 0.02 \text{ d}^{-1}$ and $0.10 \pm 0.02 \text{ d}^{-1}$, respectively (Table 2). Dissolved phosphate
9 was not detected in the U-amended controls or the pH 7.0 nitrate-amended reactors
10 without G2P (Figure 1H). However, in all G2P-containing reactors at pH 5.5, up to 120
11 μM inorganic phosphate accumulated after 30 days of incubation followed by a slow
12 linear decrease to 50 μM by day 70 (Figure 1G). Alternatively, in all pH 7.0 G2P-
13 containing reactors, inorganic phosphate accumulated up to 350 μM after 39 days of
14 incubation and remained around the same concentration for the remainder of the
15 experiments (Figure 1H). This observed accumulation of phosphate is $\sim 90\%$ lower than
16 expected if mass balance with G2P consumption was conserved, indicating that at both
17 pH a significant fraction of phosphate was removed by adsorption onto the solid phase,
18 uptake by microbial populations, and/or precipitation of phosphate minerals.

19 All reactors amended with 300 μM U but not G2P at both pH initially contained
20 only 2 μM uranium in solution, and uranium concentrations remained at 2 μM for the
21 duration of the incubations (Figure 2A). As U(VI) was instantaneously removed by
22 precipitation or adsorption onto the solid phase and no temporal change in uranium
23 concentration was observed in these treatments, the pseudo-first-order rate constants for

this removal process were reported as zero (Table 2). In the presence of G2P, however, pH 5.5 reactors amended with 300 μM uranium displayed approximately 55 μM uranium in solution at time zero, while the same reactors at pH 7.0 displayed only 15 μM (Figure 2A). Rapid uranium removal to $< 0.2 \mu\text{M}$ was observed in G2P-containing reactors at pH 5.5, and U remained immobilized for the duration of the experiment regardless of the type and presence of terminal electron acceptor (TEA) (Figure 2A). Interestingly, uranium removal at pH 5.5 was divided into two distinct phases, an initial phase between 0 and 4 days during which U(VI) removal occurred with an average pseudo-first-order rate constant of $0.41 \pm 0.12 \text{ d}^{-1}$ for all treatments, and a second phase between 7 and 30 days during which removal occurred with an average pseudo-first-order rate constant $0.10 \pm 0.02 \text{ d}^{-1}$ for all treatments (Table 2, Figure 2B). In contrast, the initial 15 μM uranium present in pH 7.0 reactors was steadily titrated out of solution over the 70 day sampling period to $< 0.2 \mu\text{M}$ (Figure 2A) with a pseudo-first-order rate constant of $0.06 \pm 0.01 \text{ d}^{-1}$ (Table 2) regardless of the presence or absence of elevated sulfate concentrations.

3.2 Solid-phase speciation of uranium and phosphate

A total phosphate concentration of $4.4 \pm 0.7 \mu\text{mol P g}^{-1}$ was extracted in the original sediment prior to phosphate amendment. Not surprisingly, solid phase extractions of sediments revealed higher total extracted phosphate in all G2P-containing reactors than in reactors without G2P (Figure 3A-B). As expected, phosphate was not detected in the exchangeable fraction (Figure 3A-B), as phosphate should not exchange with Mg^{2+} . Without G2P, extracted phosphate was primarily concentrated in the residual fraction (Figure 3A-3B). In the presence of G2P, however, the distribution of extracted

phosphate shifted towards hydroxylamine- and peroxide-extracted fractions and was not significantly affected by the pH and the presence or type of amended TEA (Figure 3A-B). As the organophosphate compound was in great excess of uranium in these incubations, the acetate-extractable phosphate fraction, which is representative of uranium-phosphate minerals, was relatively small in all reactors compared to the other treatments (Figure 3A-B).

The original unamended sediment contained a total concentration of $0.7 \pm 0.0 \mu\text{mol U g}^{-1}$ soil or about 25% of the total extracted uranium after amendments of $300 \mu\text{M U(VI)}$. The acetate extractable uranium fraction constituted the largest fraction ($\sim 60\%$) of total extracted uranium in all reactor treatments, regardless of the pH (Figure 4A-B), followed by the hydroxylamine extractable fraction ($\sim 30\%$) as the second most abundant. Except for the exchangeable fraction in the pH 5.5 U-amended controls, other fractions did not contribute significantly to total extracted uranium (Figure 4A-B). Mass-balance on uranium from sequential extractions was respected (within error) in each treatment except for pH 7.0 reactors amended with G2P but no TEA ($80.1 \pm 11.5 \%$) and pH 7.0 reactors amended with 5 mM NO_3^- but no G2P ($116.8 \pm 9.9 \%$) (Figure 4A-B). Further bulk characterization of solid-associated uranium by XAS provided information on the oxidation state and speciation of uranium in each reactor. The normalized and background-subtracted solid phase XANES spectra of samples from each treatment exhibited a uranium L_{III} -edge at $\sim 17163 \text{ eV}$ and a characteristic U(VI) shoulder between 17188 and 17200 eV , regardless of pH, indicating U(VI) as the main oxidation state of uranium in these systems (Figures 5A and 6A). In all pH 5.5 reactors, the k^3 -weighted EXAFS fittings confirmed the presence of an axial oxygen shell at 1.80 \AA (Figure 5B-C,

Table 3). In addition, two distinct equatorial oxygen shells were evidenced which may be grouped into two subsets based on radial distance (R) from the central uranium atom. The first equatorial oxygen group clustered at approximately 2.30 Å with coordination numbers between 2.3 and 3.5. The second equatorial oxygen group clustered at approximately 2.45 Å with coordination numbers between 1.9 and 3.4. As expected at pH 5.5, carbon from carbonates was not found in the neighborhood of uranium in any reactor. In contrast, Mn and/or Fe shells between 3 and 3.5 Å were necessary in all pH 5.5 reactors to improve the fit. Finally, phosphorus shells at ~ 3.65 Å improved the fit in the G2P-amended reactors without external TEA (day 70) and in the presence of excess sulfate (day 70) and nitrate (T = 70).

As observed at pH 5.5, the k^3 -weighted EXAFS fittings of pH 7.0 sediments confirmed the presence of an axial oxygen shell at 1.83 Å (Figure 6B-C, Table 4). Similarly, two distinct equatorial oxygen shells were also observed in all pH 7.0 reactors. The first equatorial oxygen group clustered at approximately 2.25 Å with coordination numbers between 1.4 and 2.0, and the second equatorial oxygen group clustered at approximately 2.42 Å with coordination numbers between 1.6 and 3.7. As expected at pH 7.0, carbon was needed to improve the fit in the nitrate-amended reactors and the sulfate-amended reactors. Similarly, Mn and/or Fe shells between 3.2 and 3.5 Å were necessary in the pH 7.0 reactors to improve the fit. Finally, phosphorus shells at ~ 3.65 Å improved the fit in the G2P-amended reactors only.

4. DISCUSSION

Both U(VI) bioreduction and the biomineralization of U(VI)-phosphate minerals are potentially viable approaches to immobilize uranium in contaminated subsurfaces.

1 Bioreduction in low pH soils is typically promoted by buffering the pH to circumneutral
2 values and introducing an electron donor, and U(VI) reduction usually occurs after
3 complete reduction of nitrate (Madden et al., 2009; Nyman et al., 2006; Wu et al.,
4 2006b) and may be concurrent with sulfate or iron reduction (Akob et al., 2008; Cardenas
5 et al., 2010; Madden et al., 2009; Nyman et al., 2006). Biomineralization of U(VI)-
6 phosphate minerals preferentially occurs in low to circumneutral pH conditions in both
7 anaerobic and aerobic environments, provided that organophosphates are available
8 (Beazley et al., 2007, 2009; Beazley et al., 2011; Macaskie et al., 1995; Martinez et al.,
9 2007; Montgomery et al., 1995; Shelobolina et al., 2009). Although these processes
10 potentially overlap in reducing conditions, the competition dynamic between adsorption,
11 U(VI)-phosphate biomineralization, and bioreduction has yet to be examined. To
12 determine which anaerobic respiration process is most conducive to uranium removal
13 through U(VI)-phosphate biomineralization and whether bioreduction can compete with
14 biomineralization in G2P-amended sediments, this study investigated the relationship
15 between these competing processes at pH 5.5 and 7.0 in the presence of iron oxides and
16 elevated concentrations of sulfate or nitrate as terminal electron acceptors and G2P as the
17 organophosphate source for U(VI)-phosphate biomineralization.

18 **4.1 Terminal electron acceptor transformations**

19 Although a variety of sulfate-reducing bacteria have been detected in ORFRC
20 wells (Cardenas et al., 2010; Gihring et al., 2011), no evidence of sulfate reduction was
21 observed in any treatment regardless of the presence or absence of G2P and pH
22 conditions (Figure 1A-B): sulfate concentrations remained steady in all reactors, even
23 after complete removal of nitrate and in the presence of elevated sulfate concentrations;

1 the sediments remained brown, characteristic of the high iron content of ORFRC
2 sediments, throughout the course of the experiment; and sulfide odors were not noticed.
3 These findings are not consistent with past studies conducted with Oak Ridge sediments
4 that observed substantial sulfate reduction after the system pH was raised to between 6.0
5 and 7.5 (Akob et al., 2008; Gu et al., 2005; Kelly et al., 2009; Kim et al., 2010; Madden
6 et al., 2009; Wu et al., 2006b; Zhang et al., 2010). Electron donor limitations may have
7 prevented sulfate reduction from occurring, as G2P represented the only carbon source
8 added to these incubations. Ambiguous information is available on the ability of sulfate
9 reducers to metabolize or assimilate glycerol, the by-product of G2P hydrolysis. Even
10 though sulfate reduction coupled to glycerol oxidation was observed in acidic sediments
11 conditioned by acid mine drainage (Becerra et al., 2009), sulfate reduction is known to be
12 highly electron donor dependent (Madden et al., 2009; Petrie et al., 2003), suggesting that
13 glycerol may have limited the activity of sulfate-reducing bacteria.

14 Alternately, the background nitrate concentrations in the present study, reflective
15 of the high nitrate levels at the ORFRC, may have prevented stimulation of sulfate-
16 reducing bacteria. Nitrate-reducing bacteria are diverse and active in ORFRC soils
17 (Spain and Krumholz, 2011), and a subset of the nitrate reducers that are metabolically
18 active include members of the genera *Burkholderia*, *Ralstonia*, *Castellaniella*,
19 *Herbaspirillum*, *Dechloromonas*, *Zooglea*, *Rhodanobacter*, *Rhizobiaceae*,
20 *Sphingomonas*, *Magnetospirillum*, and *Paenibacillus* (Akob et al., 2007; Green et al.,
21 2010; Green et al., 2012; Mohanty et al., 2008). In addition, *Rahnella* sp. Y9602, a
22 phosphatase-positive metal-resistant bacterium isolated from ORFRC soils (Martinez et
23 al., 2006), is able to reduce nitrate anaerobically while promoting biomineralization of

U(VI)-phosphate minerals (Beazley et al., 2009). The results of the present study confirm that G2P addition is sufficient to stimulate nitrate reduction by indigenous nitrate reducing bacteria of ORFRC sediments in varied pH conditions and variable nitrate concentrations (Figure 1C-D). The higher pseudo first-order rate constant at pH 7.0 compared to pH 5.5 (Table 2) indicates that nitrate reduction was more efficient at circumneutral pH, which is consistent with previous findings at the ORFRC (Edwards et al., 2007; Istok et al., 2004; Shelobolina et al., 2003). Simultaneously, only ephemeral nitrite accumulation was observed in incubations amended with G2P only and both G2P and sulfate regardless of pH (Figure 1C-D), likely due to further reduction of nitrite to other denitrification products or ammonia during dissimilatory nitrate reduction to ammonia (DNRA) (Herbert, 1999). In turn, 4 mM NO_2^- accumulated in pH 5.5 nitrate-amended reactors (Figure 1C), and comparison of nitrate reduction rates ($-180.9 \pm 11.6 \mu\text{M d}^{-1}$) and net nitrite production rates at pH 5.5 ($157.3 \pm 4.7 \mu\text{M d}^{-1}$) suggests denitrification or DNRA removed nitrite from this reactor at a rate of $-23.6 \pm 12.5 \mu\text{M d}^{-1}$.

The accumulation of high NO_2^- concentrations in the pH 5.5 nitrate-amended reactors may also have had a toxic effect on denitrifying bacteria that is reflected in a decrease in the pseudo-first-order rate constant for nitrate reduction in nitrate-amended reactors compared to G2P-amended and sulfate-amended reactors (Table 2). The nitrite toxicity effect is well documented and is evidenced in a wide variety of microorganisms. Proposed mechanisms include an increase in the permeability of the cytoplasmic membrane (Sijbesma et al., 1996) and the disruption of proton translocation stoichiometry (Rake and Eagon, 1980). In addition, elevated levels of nitrite have been

1 shown to interfere with denitrification pathways, a phenomenon that is known to be
2 exaggerated in anaerobic conditions (Bollag and Henninger, 1978; Meijer et al., 1979).
3 These findings suggest that the accumulation of NO_2^- in the pH 5.5 nitrate-amended
4 reactors may have resulted from the toxicity of NO_2^- on nitrite-reducing bacteria, while
5 the relatively minimal NO_2^- concentrations detected in other incubations were likely not
6 significant to affect nitrite-reducing bacteria.

7 Iron reduction was not significantly inhibited by elevated nitrate concentrations
8 (Figure 1C-F) in contrast to what is known about the inhibitory effect of nitrate on iron
9 reduction (Dichristina, 1992; Finneran et al., 2002a; Finneran et al., 2002b; Senko et al.,
10 2002). In addition, iron reduction was unaffected by the presence of G2P (Figure 1E-F).
11 However, a significant inhibition on iron reduction was apparent at pH 5.5 (Figure 1E),
12 consistent with previous findings demonstrating that microbial growth is impacted in low
13 pH conditions (Edwards et al., 2007). As Fe^{2+} production preceded nitrate removal and
14 production of nitrite, chemical reduction of Fe^{3+} coupled to reoxidation of nitrite was
15 likely not significant, and the observed production of Fe^{2+} was likely due to microbially-
16 mediated G2P-independent iron reduction in the presence of nitrate (Figure 1C-F). These
17 observations suggest that iron-reducing bacteria present at the ORFRC may be active in
18 nutrient- and electron donor-limited environments when nitrate-reducing bacteria remain
19 dormant.

20 The rapid rise and decrease of adsorbed Fe^{2+} not balanced by accumulation of
21 dissolved Fe^{2+} in all reactors regardless of pH (Figure 1E-F) suggests that Fe^{2+} was not
22 desorbed via an ion exchange process and instead precipitated as a distinct mineral.
23 XANES spectra confirmed the bulk oxidation state of uranium as U(VI) in all reactors

(Figures 5A and 6A), suggesting the chemical oxidation of sorbed Fe^{2+} by U(VI) (Liger et al., 1999) was likely not significant at pH 7.0 or inhibited at pH 5.5. As thermodynamic calculations predicted little adsorption of Fe^{2+} at pH 5.5 (Table 5), the observed adsorption of Fe^{2+} in all reactor treatments may have been driven by formation of ternary $=\text{Fe}-\text{OPO}_3-\text{Fe}^+$ complexes with iron oxides. These complexes are well known to occur under both pH conditions and are thought to be precursors to the surface precipitation of iron phosphate minerals even in undersaturated conditions (Ler and Stanforth, 2003; Li and Stanforth, 2000), but they were not included in the thermodynamic model. Thus, despite the fact that equilibrium calculations predict undersaturation of vivianite $[\text{Fe}_3(\text{PO}_4)_2]$ at both pHs in the conditions of the incubations (Table 5), the decrease in total Fe^{2+} coinciding with the accumulation of inorganic phosphate in solution (Figure 1E-H) could be explained by the formation of ternary iron phosphate complexes and subsequent surface-catalyzed precipitation of vivianite. This process should be investigated in future studies.

4.2 Organophosphate Hydrolysis

Incubations in the presence of G2P clearly illustrate that organophosphate hydrolysis is significant in reducing conditions (Figure 1G-H) and stimulates anaerobic respiration (Figure 1C-D) compared to otherwise identical control incubations without G2P. The distribution of phosphate extracted simultaneously with uranium from the solid phase at the end of the incubations demonstrates that phosphate exists primarily in highly recalcitrant phases in the absence of organophosphate (Figure 3A-B), suggesting that anaerobic respiration is limited by the availability of phosphorus in these conditions. In contrast, the distribution of solid-phase associated phosphate shifts towards more reactive

1 phases in the presence of G2P (Figure 3A-B). These findings imply the supply of labile
2 organic carbon (i.e. glycerol) or phosphate to support the metabolism and growth of the
3 indigenous microbial community represents the driving force for G2P hydrolysis.
4 Previous studies have demonstrated glycerol oxidation coupled to iron (Petrie et al.,
5 2003), sulfate (Qatibi et al., 1991), and uranium (Madden et al., 2007) reduction, while
6 organophosphate hydrolysis by bacterially-derived phosphatase enzymes is thought to
7 provide inorganic phosphorus either for nutrient assimilation or as a heavy-metal
8 detoxification mechanism (Macaskie et al., 1992). As uranium reduction was not favored
9 in these incubations and as G2P consumption in reactors amended with G2P was so
10 intense (1.2-2.4 mM, Figure 1G-H) compared to the availability of uranium (300 μ M) in
11 these sediments, G2P was likely hydrolyzed by bacterially-derived phosphatases
12 produced due to phosphorus or carbon limitations. In addition, G2P hydrolysis may have
13 been enhanced at pH 7.0 (Table 2) in response to the decrease in adsorption of G2P onto
14 iron oxides due to the repulsion between partially deprotonated iron oxides and totally
15 deprotonated G2P at that pH. As nitrate reduction is clearly promoted by the presence of
16 G2P in solution compared to the unamended control (Figure 1D), the decrease in G2P
17 adsorption and associated increase in G2P hydrolysis at pH 7.0 may have also promoted
18 the increase in the pseudo-first order rate constants for nitrate reduction observed at
19 circumneutral pH in the incubations amended with G2P compared to at pH 5.5 (Table 2).
20 Indeed, factoring out initial concentration of G2P from the pseudo-first order rate
21 constants reveals similar rate constants for nitrate reduction at both pH 5.5 and 7.0 (not
22 shown). Finally, the disparity between G2P consumption and phosphate production in
23 solution in all G2P-containing reactors (Figure 1G-H) indicates the existence of a

significant phosphate removal mechanism other than U(VI)-phosphate biomineralization. Thermodynamic modeling suggests ~ 80% phosphate removal through adsorption in these incubations at both pH 5.5 and 7.0 (Table 5), and solid-phase extractions (Figure 3A-B) confirm large quantities of phosphate associated with iron and manganese oxides in these sediments. Thus, sorption was likely primarily responsible for phosphate removal with less significant contributions from precipitation of U(VI)-phosphate minerals and assimilation by the natural microbial community.

4.3 Fate of Uranium

Although each treatment received a 300 μM U(VI) amendment, approximately 20% of uranium at pH 5.5 and less than 5% at pH 7.0 remained in solution initially in each reactor (Figure 2A). As ~ 95% of uranium removal between pH 5.5 and 7.0 is achieved through sorption in ORFRC soils (Barnett et al., 2000) and inorganic phosphate was initially unavailable to support U(VI) removal through the biomineralization of U(VI)-phosphate minerals, the initial uranium removal observed in all reactors can be attributed to adsorption. Important sorbents in ORFRC sediments include predominantly ferric and aluminum oxides (Brooks, 2001), which display a pH_{zpc} around 7.0 (Hsi and Langmuir, 1985; Langmuir, 1997; Stumm and Morgan, 1996), and in less extent manganese oxides (Barnett et al., 2000), which display a pH_{zpc} ranging between 1.3 and 7.3 (Langmuir, 1997). Aluminum oxides, however, are less likely to be involved in the removal of uranium at pH greater than 4.0 in the presence of iron oxides (Zheng et al., 2003). Indeed, bulk uranium EXAFS of both pH 5.5 and pH 7.0 reactors demonstrate uranium associated with Mn and/or Fe phases (Table 3-4). At pH 5.5, U(VI) carries a positive (UO_2^{2+}) or neutral ($\text{UO}_2\text{CO}_3(\text{aq})$) charge (Table 5), making it less likely to adsorb

1 to positively charged soils than negatively charged G2P or orthophosphates which
2 strongly competes for soil sorption sites, especially given their high concentration. In
3 fact, thermodynamic modeling predicts ~ 70% adsorption of U(VI) at pH 5.5 in the
4 absence of phosphate (U-control) as compared to ~ 1% adsorption in the presence of 5
5 mM phosphate from organophosphate hydrolysis (G2P-treatments) (Table 5). At pH 7.0,
6 U(VI) is primarily present as neutral $[\text{Ca}_2\text{UO}_2(\text{CO}_3)_3]$ and negatively charged species
7 $(\text{CaUO}_2\text{CO}_3^{2-})$ (Table 5), and G2P is totally deprotonated. As evidenced by the initial
8 two-fold increase in dissolved G2P at pH 7.0 compared to pH 5.5 (Figure 1D), G2P
9 adsorbs less efficiently at pH 7.0 when surface sites shift towards more negative values.
10 Thus, the decreased sorption of G2P allows for more complete sorption of U(VI) species
11 and is reflected in the four-fold decrease in aqueous uranium at pH 7.0 versus pH 5.5
12 initially (Figure 2A). In a similar fashion, the initial adsorption of U(VI) at pH 7.0 is
13 much higher in the absence (U-control) than in the presence of organophosphate.

14 Examination of the removal of uranium as a function of time reveals interesting
15 features. At pH 5.5, two kinetically-controlled uranium removal phases are observed in
16 all G2P-containing reactors (Figure 2) in agreement with previous studies that
17 demonstrated rapid adsorption of U(VI) to ferrihydrite within the first few hours of
18 equilibration at pH 5.0 is followed by a secondary removal phase that lasts several days
19 (Waite et al., 1994). The first removal phase that occurs between 0 and 4 days could be
20 attributed to the diffusion-limited sorption of uranium in the crystal lattice of minerals or
21 pores of the soil matrix (Davis and Kent, 1990; Waite et al., 1994), as during that time
22 period hydrolysis of G2P was not significant as indicated by the relatively constant
23 concentration of G2P in solution and the lack of production of inorganic phosphates

(Figure 1G). The second phase that occurs between 4 and 40 days is attributed to the precipitation of uranium phosphate controlled by the hydrolysis of G2P, as previously demonstrated in pure cultures incubations with an organism isolated from the same site (Beazley et al., 2007 and 2009) and supported by the decrease in G2P, the simultaneous production of dissolved phosphate after a small phase lag (Figure 1G), and the thermodynamic calculations that predict precipitation of almost all uranium as autunite mineral (Table 5). In pH 7.0 reactors containing G2P, only one uranium removal phase was observed (Figure 2), suggesting that uranium carbonate complexes, the dominant form of dissolved uranium in the absence of inorganic phosphate at that pH (Table 5), do not promote the diffusion-limited removal process observed in the pH 5.5 incubations. The slightly lower pseudo-first-order rate constants calculated for the removal of uranium at pH 7.0 compared the second uranium removal phase at pH 5.5 (Table 2) may be attributed to the stabilization of uranium in solution by carbonates. Overall, these data suggest that similar U(VI) removal mechanisms were ongoing in the pH 7.0 incubations. Indeed, thermodynamic calculations predict the majority of uranium is precipitated under the form of autunite minerals (Table 5).

Bioreduction is a commonly observed removal pathway for U(VI) in anaerobic conditions. In this study, however, XANES data did not show evidence of U(VI) reduction regardless of pH, even after complete nitrate removal (Figures 5A and 6A). These findings suggest that U(VI) reduction was inhibited in these incubations. Similar results were observed in both pure culture systems and sediment microcosms. Both manganese (Liu et al., 2002) and ferrihydrite (Wielinga et al., 2000) were shown to inhibit uranium reduction by acting as competitive terminal electron acceptors in pure

1 cultures, while calcium was shown to inhibit reduction of U(VI) in pure cultures through
2 the formation of ternary Ca-UO₂-CO₃ complexes which are less energetically favorable
3 terminal electron acceptors than free uranyl ions (Brooks et al., 2003). In addition,
4 uranium reduction in ORFRC sediments commonly occurs concurrently with sulfate
5 reduction (Akob et al., 2008; Cardenas et al., 2010; Kostka and Green, 2011; Luo et al.,
6 2007; Madden et al., 2009; Nyman et al., 2006; Wu et al., 2006b). Although the exact
7 mechanism of this coupling is unknown, it has recently been suggested that the observed
8 U(VI) reduction is driven by the formation of iron sulfides and subsequent sulfide-
9 catalyzed chemical reduction of U(VI) to U(IV) (Hyun et al., 2012). As no sulfate
10 reduction was observed in the present incubations and Ca-UO₂-CO₃ aqueous species are
11 predicted to dominate the speciation of U(VI) in solution (Table 5), it is unlikely that
12 uranium reduction occurred over the experimental time scale of 70 days. Finally, the
13 chemical oxidants NO₂⁻, Fe(III), and/or possibly MnO₂, which can re-oxidize uraninite in
14 reducing conditions (Fredrickson et al., 2002; Moon et al., 2007; Senko et al., 2002;
15 Senko et al., 2005a; Senko et al., 2005b; Wan et al., 2005), were present in great excess
16 in these incubations suggesting any reduced uranium would have been destabilized.

17 The biomineralization of U(VI)-phosphate minerals represents an alternative
18 U(VI) removal mechanism and has been demonstrated in both pure culture (Beazley et
19 al., 2007; Macaskie et al., 1995; Martinez et al., 2007; Montgomery et al., 1995) and soil
20 studies (Beazley et al., 2011; Shelobolina et al., 2009). The observed G2P consumption
21 and subsequent production of inorganic phosphate support the hypothesis that U(VI)-
22 phosphate biomineralization is an important contributor to U(VI) removal in these
23 experiments, and the lack of observed uranium reduction is indicative of the formation of

1 more stable U(VI)-phosphate minerals (Beazley et al., 2007; Beazley et al., 2011;
2 Shelobolina et al., 2009). In all incubations, solid-phase extractions revealed uranium
3 primarily associated with phosphate minerals (acetate extractable fraction) and bound to
4 iron/manganese oxides (hydroxylamine extracted) (Figure 4A-B). While this was
5 expected for G2P-containing reactors, uranium in the U-amended controls was also found
6 in the acetate extractable fraction. This discrepancy is likely due to precipitation of
7 schoepite during the pH 7.0 MgCl_2 extraction step designed to desorb loosely bound
8 uranium (not shown) and does not reflect actual precipitation of U(VI)-phosphate
9 minerals in reactors unamended with G2P. Thermodynamic calculations and EXAFS data
10 support the formation of U-P minerals at both pH 5.5 and 7.0 (Table 3, 4, and 5).
11 Equilibrium calculations predict 99% of uranium precipitates under the form of autunite
12 minerals at both pHs (Table 5), even when uranium phosphate ternary complexes are
13 included in the model. Following incubation for 70 days at pH 5.5 and 7.0, the fit for all
14 G2P-containing reactors was improved by the inclusion of a U-P scattering path to the
15 EXAFS fitting (Table 4, Figure 5B). In contrast, the fit was not improved by the addition
16 of a U-P EXAFS scattering path for the sample taken from G2P-amended reactors prior
17 to incubation, supporting the hypothesis that the initial uranium removal by adsorption
18 was followed by the biomineralization of U(VI)-phosphate minerals.

19 These findings have important implications for the design and implementation of
20 uranium remediation strategies in contaminated subsurface environments. First, U(VI)
21 biomineralization promoted by G2P hydrolysis appears to outcompete U(VI)
22 bioreduction in nitrate- and iron-rich environments. Almost complete uranium removal
23 may be achieved in high nitrate conditions found at some radionuclide-contaminated sites

1 without the preconditioning steps (i.e. nitrate removal and pH adjustments) required to
2 promote U(VI) bioreduction (Wu et al., 2006a). Eliminating these conditioning steps
3 may help minimize the cost of remediation. In contrast, if sulfate-reducing
4 microorganisms are not stimulated by organophosphate addition, nor involved in
5 organophosphate hydrolysis as suggested by the findings of this study, sulfate-reducing
6 conditions promoted by endogenous electron donors should lead to formation of uraninite
7 and other U(IV) mineral products. Finally, the low phosphate levels in most subsurface
8 environments are likely to favor phosphatase activity by native subsurface microbial
9 populations. The fact that such activity occurs under both aerobic (Beazley et al., 2011;
10 Shelobolina et al., 2009) and anaerobic conditions (this study), coupled to the fact that
11 uranium phosphate minerals are highly stable in a wide range of redox conditions
12 compared to U(IV) minerals, indicate that biomineralization of U(VI)- phosphate
13 minerals may be particularly useful at contaminated sites subject to fluctuating redox
14 conditions.

15 **5. CONCLUSIONS**

16 The instability of uraninite, even under reducing conditions, generates the need
17 for an alternative bioremediation strategy to decrease the solubility of uranium in
18 contaminated environments. Biomineralization of U(VI)-phosphate minerals, a possible
19 complementary technique to bioreduction, has been shown to be applicable in both
20 reducing and oxidizing environments, and the ability of ORFRC microbial isolates to
21 metabolize G2P in aerobic conditions has been demonstrated. In this study, the
22 competition dynamic between U(VI) bioreduction, U(VI)-phosphate biomineralization,
23 and adsorption in the presence of G2P and alternate terminal electron acceptors was

1 studied in anaerobically-maintained ORFRC contaminated sediments at two different
2 pHs to determine which respiratory process is promoted by G2P in these sediments and
3 its influence on the fate of uranium.

4 The addition of G2P to ORFRC Area 3 sediments was sufficient to stimulate
5 reduction of nitrate at both pH 5.5 and 7.0 but not sulfate, even after complete removal of
6 nitrate, suggesting the lack of a suitable electron donor for sulfate-reducing bacteria in
7 these incubations. Although more efficient at pH 7.0, anaerobic respiration of iron oxides
8 occurred at both pHs, even in the presence of high nitrate concentrations, and appeared to
9 be unaffected by the addition of G2P. In turn, nitrate reduction depended on G2P
10 hydrolysis and was enhanced at circumneutral pH, suggesting that G2P availability in the
11 dissolved phase may control the intensity of anaerobic nitrate respiration in these
12 sediments. High nitrate reduction rates simultaneously impacted nitrite-reducing
13 microorganisms significantly, likely via accumulation of the toxic nitrite in solution.
14 Hydrolysis of G2P was much more significant than the availability of uranium at both
15 pHs, suggesting that the hydrolysis of organophosphate in these sediments was activated
16 by phosphate or carbon limitations rather than a uranium detoxification mechanism.
17 Finally, almost complete removal of uranium through a combination of adsorption and
18 precipitation of uranium phosphate minerals was observed at both pHs. Overall, the
19 results of this study not only suggest that biomineralization of U(VI)-phosphate minerals
20 may be complementary to bioreduction, but also that U(VI)-phosphate biomineralization
21 may be preferable to bioreduction in certain environments due to its utility in a wide
22 range of chemical and redox conditions.

1
2
3
4
5
6
7
8
9
10
11
12
13
14
15
16

ACKNOWLEDGEMENTS

This research was supported by the Office of Science (BER), US Department of Energy Grant No. DE-FG02-04ER63906. Portions of this research were carried out at the Stanford Synchrotron Radiation Lightsource, a national user facility operated by Stanford University on behalf of the US Department of Energy, Office of Basic Energy Sciences. The SSRL Structural Molecular Biology Program is supported by the Department of Energy, Office of Biological and Environmental Research, and by the National Institutes of Health, National Center for Research Resources, Biomedical Technology Program. We thank Dave Watson of Oak Ridge National Laboratory for providing ORFRC sediment cores and Eric Roden for providing thermodynamic stability constants of glycerol phosphate adsorption onto iron oxides.

REFERENCES

- Akob, D.M., Mills, H.J., Gihring, T.M., Kerkhof, L., Stucki, J.W., Anastacio, A.S., Chin, K.J., Kusel, K., Palumbo, A.V., Watson, D.B., Kostka, J.E., 2008. Functional diversity and electron donor dependence of microbial populations capable of U(VI) reduction in radionuclide-contaminated subsurface sediments. *Applied and Environmental Microbiology* 74, 3159-3170.
- Akob, D.M., Mills, H.J., Kostka, J.E., 2007. Metabolically active microbial communities in uranium-contaminated subsurface sediments. *Fems Microbiology Ecology* 59, 95-107.
- Allen, P.G., Shuh, D.K., Bucher, J.J., Edelstein, N.M., Palmer, C.E.A., Silva, R.J., Nguyen, S.N., Marquez, L.N., Hudson, E.A., 1996. Determinations of uranium structures by EXAFS: Schoepite and other U(VI) oxide precipitates. *Radiochimica Acta* 75, 47-53.
- Ankudinov, A.L., Ravel, B., Rehr, J.J., Conradson, S.D., 1998. Real-space multiple-scattering calculation and interpretation of x-ray-absorption near-edge structure. *Physical Review B* 58, 7565.
- Appelo, C.A.J., Van der Weiden, M.J.J., Tournassat, C., Charlet, L., 2002. Surface complexation of ferrous iron and carbonate on ferrihydrite and the mobilization of arsenic. *Environmental Science & Technology* 36, 3096-3103.
- Arai, Y., Marcus, M.K., Tamura, N., Davis, J.A., Zachara, J.M., 2007. Spectroscopic evidence for uranium bearing precipitates in vadose zone sediments at the Hanford 300-area site. *Environmental Science & Technology* 41, 4633-4639.

- 1 Bak, W.a., 1992. Gram-negative mesophilic sulfate-reducing bacteria, in: A. Balows,
2 H.G.T., M. Dworkin, W. Harder, and K.-H. Schleifer (Ed.), *The Prokaryotes*, 2
3 ed. Springer, New York, pp. 3352-3378.
- 4 Bargar, J.R., Reitmeyer, R., Lenhart, J.J., Davis, J.A., 2000. Characterization of U(VI)-
5 carbonato ternary complexes on hematite: EXAFS and electrophoretic mobility
6 measurements. *Geochimica Et Cosmochimica Acta* 64, 2737-2749.
- 7 Barnett, M.O., Jardine, P.M., Brooks, S.C., 2002. U(VI) adsorption to heterogeneous
8 subsurface media: Application of a surface complexation model. *Environmental*
9 *Science & Technology* 36, 937-942.
- 10 Barnett, M.O., Jardine, P.M., Brooks, S.C., Selim, H.M., 2000. Adsorption and transport
11 of uranium(VI) in subsurface media. *Soil Science Society of America Journal* 64,
12 908-917.
- 13 Beazley, M.J., Martinez, R.J., Sobecky, P.A., Webb, S.M., Taillefert, M., 2007. Uranium
14 biomineralization as a result of bacterial phosphatase activity: Insights from
15 bacterial isolates from a contaminated subsurface. *Environmental Science &*
16 *Technology* 41, 5701-5707.
- 17 Beazley, M.J., Martinez, R.J., Sobecky, P.A., Webb, S.M., Taillefert, M., 2009.
18 Nonreductive Biomineralization of Uranium(VI) Phosphate Via Microbial
19 Phosphatase Activity in Anaerobic Conditions. *Geomicrobiology Journal* 26, 431-
20 441.
- 21 Beazley, M.J., Martinez, R.J., Webb, S.M., Sobecky, P.A., Taillefert, M., 2011. The
22 effect of pH and natural microbial phosphatase activity on the speciation of
23 uranium in subsurface soils. *Geochimica Et Cosmochimica Acta* 75, 5648-5663.

- 1 Becerra, C.A., Lopez-Luna, E.L., Ergas, S.J., Nuesslein, K., 2009. Microcosm-based
2 Study of the Attenuation of an Acid Mine Drainage-Impacted Site through
3 Biological Sulfate and Iron Reduction. *Geomicrobiology Journal* 26, 9-20.
- 4 Behrends, T., Van Cappellen, P., 2005. Competition between enzymatic and abiotic
5 reduction of uranium(VI) under iron reducing conditions. *Chemical Geology* 220,
6 315-327.
- 7 Beller, H.R., 2005. Anaerobic, nitrate-dependent oxidation of U(IV) oxide minerals by
8 the chemolithoautotrophic bacterium *Thiobacillus denitrificans*. *Applied and*
9 *Environmental Microbiology* 71, 2170-2174.
- 10 Bernier-Latmani, R., Veeramani, H., Vecchia, E.D., Junier, P., Lezama-Pacheco, J.S.,
11 Suvorova, E.I., Sharp, J.O., Wigginton, N.S., Bargar, J.R., 2010. Non-uraninite
12 Products of Microbial U(VI) Reduction. *Environmental Science & Technology*
13 44, 9456-9462.
- 14 Beyenal, H., Sani, R.K., Peyton, B.M., Dohnalkova, A.C., Amonette, J.E., Lewandowski,
15 Z., 2004. Uranium immobilization by sulfate-reducing biofilms. *Environmental*
16 *Science & Technology* 38, 2067-2074.
- 17 Blakeney, M.D., Moulaei, T., DiChristina, T.J., 2000. Fe(III) reduction activity and
18 cytochrome content of *Shewanella putrefaciens* grown on ten compounds as sole
19 terminal electron acceptor. *Microbiological Research* 155, 87-94.
- 20 Bollag, J.M., Henninger, N.M., 1978. Effects of nitrite toxicity on soil bacteria under
21 aerobic and anaerobic conditions. *Soil Biology & Biochemistry* 10, 377-381.

1 Brooks, S.C., 2001. Waste Characteristics of the Former S-3 Ponds and Outline of
2 Uranium Chemistry Relevant to NABIR Field Research Center Studies. NABIR
3 FRC.

4 Brooks, S.C., Fredrickson, J.K., Carroll, S.L., Kennedy, D.W., Zachara, J.M., Plymale,
5 A.E., Kelly, S.D., Kemner, K.M., Fendorf, S., 2003. Inhibition of bacterial U(VI)
6 reduction by calcium. *Environmental Science & Technology* 37, 1850-1858.

7 Cardenas, E., Wu, W.-M., Leigh, M.B., Carley, J., Carroll, S., Gentry, T., Luo, J.,
8 Watson, D., Gu, B., Ginder-Vogel, M., Kitanidis, P.K., Jardine, P.M., Zhou, J.,
9 Criddle, C.S., Marsh, T.L., Tiedje, J.M., 2010. Significant Association between
10 Sulfate-Reducing Bacteria and Uranium-Reducing Microbial Communities as
11 Revealed by a Combined Massively Parallel Sequencing-Indicator Species
12 Approach. *Appl. Environ. Microbiol.* 76, 6778-6786.

13 Catalano, J.G., McKinley, J.P., Zachara, J.M., Heald, S.M., Smith, S.C., Brown, G.E.,
14 2006. Changes in uranium speciation through a depth sequence of contaminated
15 Hanford sediments. *Environmental Science & Technology* 40, 2517-2524.

16 Chakraborty, S., Favre, F., Banerjee, D., Scheinost, A.C., Mullet, M., Ehrhardt, J.-J.,
17 Brendle, J., Vidal, L., Charlet, L., 2010. U(VI) Sorption and Reduction by Fe(II)
18 Sorbed on Montmorillonite. *Environmental Science & Technology* 44, 3779-
19 3785.

20 Cheng, T., Barnett, M.O., Roden, E.E., Zhuang, J.L., 2004. Effects of phosphate on
21 uranium(VI) adsorption to goethite-coated sand. *Environmental Science &*
22 *Technology* 38, 6059-6065.

- 1 Davis, J.A., Kent, D.B., 1990. Surface Complexation Modeling in Aqueous
2 Geochemistry. *Reviews in Mineralogy* 23, 177-260.
- 3 Dawson, G.W., Gilman, J., 2001. Land reclamation technology - expanding the
4 geotechnical engineering envelope. *Proceedings of the Institution of Civil
5 Engineers-Geotechnical Engineering* 149, 49-61.
- 6 De Pablo, J., Casas, I., Gimenez, J., Molera, M., Rovira, M., Duro, L., Bruno, J., 1999.
7 The oxidative dissolution mechanism of uranium dioxide. I. The effect of
8 temperature in hydrogen carbonate medium. *Geochimica Et Cosmochimica Acta*
9 63, 3097-3103.
- 10 Dichristina, T.J., 1992. Effects of nitrate and nitrite on dissimilatory iron reduction by
11 *shewanella-putrefaciens*-200. *Journal of Bacteriology* 174, 1891-1896.
- 12 DOE, 1997. Linking Legacies - Connecting the Cold War Nuclear Weapons Production
13 Processes to Their Environmental Consequences Office of Environmental
14 Management - The U.S. Department of Energy Washington, D.C.
- 15 Dong, W.M., Brooks, S.C., 2006. Determination of the formation constants of ternary
16 complexes of uranyl and carbonate with alkaline earth metals (Mg^{2+} , Ca^{2+} , Sr^{2+} ,
17 and Ba^{2+}) using anion exchange method. *Environmental Science & Technology*
18 40, 4689-4695.
- 19 Edwards, L., Kusel, K., Drake, H., Kostka, J.E., 2007. Electron flow in acidic subsurface
20 sediments co-contaminated with nitrate and uranium. *Geochimica Et
21 Cosmochimica Acta* 71, 643-654.
- 22 Finch, R., Murakami, T., 1999. Systematics and paragenesis of uranium minerals.
23 *Reviews in Mineralogy and Geochemistry* 38, 91-179.

1 Finneran, K.T., Anderson, R.T., Nevin, K.P., Lovley, D.R., 2002a. Potential for
2 Bioremediation of uranium-contaminated aquifers with microbial U(VI)
3 reduction. *Soil & Sediment Contamination* 11, 339-357.

4 Finneran, K.T., Housewright, M.E., Lovley, D.R., 2002b. Multiple influences of nitrate
5 on uranium solubility during bioremediation of uranium-contaminated subsurface
6 sediments. *Environmental Microbiology* 4, 510-516.

7 Fletcher, K.E., Boyanov, M.I., Thomas, S.H., Wu, Q.Z., Kemner, K.M., Löffler, F.E.,
8 2010. U(VI) Reduction to Mononuclear U(IV) by *Desulfitobacterium* Species.
9 *Environmental Science & Technology* 44, 4705-4709.

10 Fox, P.M., Davis, J.A., Zachara, J.M., 2006. The effect of calcium on aqueous
11 uranium(VI) speciation and adsorption to ferrihydrite and quartz. *Geochimica Et*
12 *Cosmochimica Acta* 70, 1379-1387.

13 Fredrickson, J.K., Zachara, J.M., Kennedy, D.W., Duff, M.C., Gorby, Y.A., Li, S.M.W.,
14 Krupka, K.M., 2000. Reduction of U(VI) in goethite (α -FeOOH) suspensions
15 by a dissimilatory metal-reducing bacterium. *Geochimica Et Cosmochimica Acta*
16 64, 3085-3098.

17 Fredrickson, J.K., Zachara, J.M., Kennedy, D.W., Liu, C.X., Duff, M.C., Hunter, D.B.,
18 Dohnalkova, A., 2002. Influence of Mn oxides on the reduction of uranium(VI)
19 by the metal-reducing bacterium *Shewanella putrefaciens*. *Geochimica Et*
20 *Cosmochimica Acta* 66, 3247-3262.

21 Ganesh, R., Robinson, K.G., Chu, L.L., Kucsmas, D., Reed, G.D., 1999. Reductive
22 precipitation of uranium by *Desulfovibrio desulfuricans*: Evaluation of
23 cocontaminant effects and selective removal. *Water Research* 33, 3447-3458.

1 Gihring, T.M., Zhang, G., Brandt, C.C., Brooks, S.C., Campbell, J.H., Carroll, S.,
 2 Criddle, C.S., Green, S.J., Jardine, P., Kostka, J.E., Lowe, K., Mehlhorn, T.L.,
 3 Overholt, W., Watson, D.B., Yang, Z., Wu, W.-M., Schadt, C.W., 2011. A
 4 Limited Microbial Consortium Is Responsible for Extended Bioreduction of
 5 Uranium in a Contaminated Aquifer. *Applied and Environmental Microbiology*
 6 77, 5955-5965.

7 Gleyzes, C., Tellier, S., Astruc, M., 2002. Fractionation studies of trace elements in
 8 contaminated soils and sediments: a review of sequential extraction procedures.
 9 *Trac-Trends in Analytical Chemistry* 21, 451-467.

10 Grasshoff, K., 1983. Determination of Nitrite, in: Grasshoff, K., Ehrhardt, M., Kremling,
 11 K., Almgren, T. (Eds.), *Methods of seawater analysis*, 2nd, rev. and extended ed.
 12 ed. Verlag Chemie GmbH, Weinheim

13 Green, S.J., Prakash, O., Gihring, T.M., Akob, D.M., Jasrotia, P., Jardine, P.M., Watson,
 14 D.B., Brown, S.D., Palumbo, A.V., Kostka, J.E., 2010. Denitrifying Bacteria
 15 Isolated from Terrestrial Subsurface Sediments Exposed to Mixed-Waste
 16 Contamination. *Applied and Environmental Microbiology* 76, 3244-3254.

17 Green, S.J., Prakash, O., Jasrotia, P., Overholt, W.A., Cardenas, E., Hubbard, D., Tiedje,
 18 J.M., Watson, D.B., Schadt, C.W., Brooks, S.C., Kostka, J.E., 2012. Denitrifying
 19 Bacteria from the Genus *Rhodanobacter* Dominate Bacterial Communities in the
 20 Highly Contaminated Subsurface of a Nuclear Legacy Waste Site. *Applied and*
 21 *Environmental Microbiology* 78, 1039-1047.

1 Gu, B.H., Wu, W.M., Ginder-Vogel, M.A., Yan, H., Fields, M.W., Zhou, J., Fendorf, S.,
2 Criddle, C.S., Jardine, P.M., 2005. Bioreduction of uranium in a contaminated soil
3 column. *Environmental Science & Technology* 39, 4841-4847.

4 Guillaumont, R., Fanghänel, T., Fuger, J., Grenthe, I., Neck, V., Palmer, D.A., Rand,
5 M.H., 2003. *Chemical Thermodynamics 5. Update on the Chemical*
6 *Thermodynamics of Uranium, Neptunium, Plutonium, Americium and*
7 *Technetium*. Elsevier, Amsterdam.

8 Han, R.P., Zou, W.H., Wang, Y., Zhu, L., 2007. Removal of uranium(VI) from aqueous
9 solutions by manganese oxide coated zeolite: discussion of adsorption isotherms
10 and pH effect. *Journal of Environmental Radioactivity* 93, 127-143.

11 Herbert, R.A., 1999. Nitrogen cycling in coastal marine ecosystems. *Fems Microbiology*
12 *Reviews* 23, 563-590.

13 Ho, C.H., Miller, N.H., 1986. Formation of uranium oxide sols in bicarbonate solutions
14 *Journal of Colloid and Interface Science* 113, 232-240.

15 Hsi, C.K.D., Langmuir, D., 1985. Adsorption of uranyl onto ferric oxyhydroxides -
16 Application of the surface complexation site-binding model. *Geochimica Et*
17 *Cosmochimica Acta* 49, 1931-1941.

18 Hudson, E.A., Allen, P.G., Terminello, L.J., Denecke, M.A., Reich, T., 1996. Polarized
19 x-ray-absorption spectroscopy of the uranyl ion: Comparison of experiment and
20 theory. *Physical Review B* 54, 156.

21 Hyun, S.P., Davis, J.A., Sun, K., Hayes, K.F., 2012. Uranium(VI) Reduction by Iron(II)
22 Monosulfide Mackinawite. *Environmental Science & Technology* 46, 3369-3376.

1 Istok, J.D., Senko, J.M., Krumholz, L.R., Watson, D., Bogle, M.A., Peacock, A., Chang,
2 Y.J., White, D.C., 2004. In situ bioreduction of technetium and uranium in a
3 nitrate-contaminated aquifer. *Environmental Science & Technology* 38, 468-475.

4 Jardine, P.M., Watson, D.B., Blake, D.A., Beard, L.P., Brooks, S.C., Carley, J.M.,
5 Criddle, C.S., Doll, W.E., Fields, M.W., Fendorf, S.E., Geesey, G.G., Ginder-
6 Vogel, M., Hubbard, S.S., Istok, J.D., Kelly, S., Kemner, K.M., Peacock A.D.,
7 Spalding, B.P., White, D.C., Wolfe, A., Wu, W., Zhou, J., 2006. Techniques for
8 assessing the performance of in situ bioreduction and immobilization of metals
9 and radionuclides in contaminated subsurface environments. Technical Report;
10 NABIR FRC.

11 Jeon, B.H., Dempsey, B.A., Burgos, W.D., Barnett, M.O., Roden, E.E., 2005. Chemical
12 reduction of U(VI) by Fe(II) at the solid-water interface using natural and
13 synthetic Fe(III) oxides. *Environmental Science & Technology* 39, 5642-5649.

14 Jeon, B.H., Kelly, S.D., Kemner, K.M., Barnett, M.O., Burgos, W.D., Dempsey, B.A.,
15 Roden, E.E., 2004. Microbial reduction of U(VI) at the solid-water interface.
16 *Environmental Science & Technology* 38, 5649-5655.

17 Jerden, J.L., Sinha, A.K., 2003. Phosphate based immobilization of uranium in an
18 oxidizing bedrock aquifer. *Applied Geochemistry* 18, 823-843.

19 Katsoyiannis, I.A., 2007. Carbonate effects and pH-dependence of uranium sorption onto
20 bacteriogenic iron oxides: Kinetic and equilibrium studies. *Journal of Hazardous*
21 *Materials* 139, 31-37.

22 Kelly, S.D., Kemner, K.M., O'Loughlin, E.J., Boyanov, M.I., Watson, D.B., Jardine,
23 P.M., Phillips, D.H., 2005. U L₃-Edge EXAFS Measurements of Sediment

1 Samples from Oak Ridge National Laboratory, Tennessee, U.S.A. Technical
2 Report.

3 Kelly, S.D., Wu, W.-M., Yang, F., Criddle, C.S., Marsh, T.L., O'Loughlin, E.J., Ravel,
4 B., Watson, D., Jardine, P.M., Kemner, K.M., 2009. Uranium Transformations in
5 Static Microcosms. *Environmental Science & Technology* 44, 236-242.

6 Kim, O.-H., Kim, Y.-O., Shim, J.-H., Jung, Y.-S., Jung, W.-J., Choi, W.-C., Lee, H., Lee,
7 S.-J., Kim, K.-K., Auh, J.-H., Kim, H., Kim, J.-W., Oh, T.-K., Oh, B.-C., 2010.
8 beta-Propeller Phytase Hydrolyzes Insoluble Ca(2+)-Phytate Salts and
9 Completely Abrogates the Ability of Phytate To Chelate Metal Ions.
10 *Biochemistry* 49, 10216-10227.

11 Kostka, J.E., Green, S.J., 2011. Microorganisms and processes linked to uranium
12 reduction and immobilization, in: Stolz, J.F., Oremland, R.S. (Eds.), *Microbial*
13 *Metal and Metalloid Metabolism: Advances and Applications*. ASM Press,
14 Washington, D.C., pp. 117-138.

15 Kosztolanyi, K., Nguyen, T.C., Lhote, F., Vernet, M., 1996. Reduction of uranyl
16 complexes and precipitation of uranium oxides by means of hydrogen sulphide
17 gas. *Magyar Kemiai Folyoirat* 102, 180-187.

18 Langmuir, D., 1997. *Aqueous Environmental Geochemistry*. Prentice Hall, Upper Saddle
19 River, New Jersey.

20 Ler, A., Stanforth, R., 2003. Evidence for surface precipitation of phosphate on goethite.
21 *Environmental Science & Technology* 37, 2694-2700.

1 Li, L., Stanforth, R., 2000. Distinguishing adsorption and surface precipitation of
2 phosphate on goethite (α -FeOOH). Journal of Colloid and Interface Science
3 230, 12-21.

4 Liger, E., Charlet, L., Van Cappellen, P., 1999. Surface catalysis of uranium(VI)
5 reduction by iron(II). Geochimica Et Cosmochimica Acta 63, 2939-2955.

6 Liu, C.X., Zachara, J.M., Fredrickson, J.K., Kennedy, D.W., Dohnalkova, A., 2002.
7 Modeling the inhibition of the bacterial reduction of U(VI) by beta-MnO₂(S)(g).
8 Environmental Science & Technology 36, 1452-1459.

9 Liu, C.X., Zachara, J.M., Qafoku, O., McKinley, J.P., Heald, S.M., Wang, Z.M., 2004.
10 Dissolution of uranyl microprecipitates in subsurface sediments at Hanford site,
11 USA. Geochimica Et Cosmochimica Acta 68, 4519-4537.

12 Lovley, D.R., Phillips, E.J.P., 1992. Reduction of uranium by desulfovibrio-
13 desulfuricans. Applied and Environmental Microbiology 58, 850-856.

14 Lovley, D.R., Phillips, E.J.P., Gorby, Y.A., Landa, E.R., 1991. Microbial reduction of
15 uranium Nature 350, 413-416.

16 Luo, J., Weber, F.A., Cirpka, O.A., Wu, W.M., Nyman, J.L., Carley, J., Jardine, P.M.,
17 Criddle, C.S., Kitanidis, P.K., 2007. Modeling in-situ uranium(VI) bioreduction
18 by sulfate-reducing bacteria. Journal of Contaminant Hydrology 92, 129-148.

19 Macaskie, L.E., Empson, R.M., Cheetham, A.K., Grey, C.P., Skarnulis, A.J., 1992.
20 Uranium bioaccumulation by a *citrobacter* sp as a result of enzymatically
21 mediated growth of polycrystalline H₂UO₂PO₄ Science 257, 782-784.

22 Macaskie, L.E., Hewitt, C.J., Shearer, J.A., Kent, C.A., 1995. Biomass production for the
23 removal of heavy-metals from aqueous-solutions at low pH using growth-

1 decoupled cells of a citrobacter sp. International Biodeterioration &
2 Biodegradation 35, 73-92.

3 Mackay, D.M., Cherry, J.A., 1989. Groundwater contamination: pump-and-treat
4 remediation part 2. Environmental Science & Technology 23, 630-636.

5 Madden, A.S., Palumbo, A.V., Ravel, B., Vishnivetskaya, T.A., Phelps, T.J., Schadt,
6 C.W., Brandt, C.C., 2009. Donor-dependent Extent of Uranium Reduction for
7 Bioremediation of Contaminated Sediment Microcosms. Journal of
8 Environmental Quality 38, 53-60.

9 Madden, A.S., Smith, A.C., Balkwill, D.L., Fagan, L.A., Phelps, T.J., 2007. Microbial
10 uranium immobilization independent of nitrate reduction. Environmental
11 Microbiology 9, 2321-2330.

12 Marsili, E., Beyenal, H., Di Palma, L., Merli, C., Dohnalkova, A., Amonette, J.E.,
13 Lewandowski, Z., 2007. Uranium immobilization by sulfate-reducing biofilms
14 grown on hematite, dolomite, and calcite. Environmental Science & Technology
15 41, 8349-8354.

16 Martinez, R.J., Beazley, M.J., Taillefert, M., Arakaki, A.K., Skolnick, J., Sobecky, P.A.,
17 2007. Aerobic uranium (VI) bioprecipitation by metal-resistant bacteria isolated
18 from radionuclide- and metal-contaminated subsurface soils. Environmental
19 Microbiology 9, 3122-3133.

20 Martinez, R.J., Wang, Y.L., Raimondo, M.A., Coombs, J.M., Barkay, T., Sobecky, P.A.,
21 2006. Horizontal gene transfer of P-IB-type ATPases among bacteria isolated
22 from radionuclide- and metal-contaminated subsurface soils. Applied and
23 Environmental Microbiology 72, 3111-3118.

- 1 Meijer, E.M., Vanderzwaan, J.W., Wever, R., Stouthamer, A.H., 1979. Anaerobic
2 respiration and energy-conservation in paracoccus-denitrificans - Functioning of
3 iron-sulfur centers and the uncoupling effect of nitrite. European Journal of
4 Biochemistry 96, 69-76.
- 5 Meleshyn, A., Azeroual, M., Reeck, T., Houben, G., Riebe, B., Bunnenberg, C., 2009.
6 Influence of (Calcium-)Uranyl-Carbonate Complexation on U(VI) Sorption on
7 Ca- and Na-Bentonites. Environmental Science & Technology 43, 4896-4901.
- 8 Mohagheghi, A., Updegraff, D.M., Goldhaber, M.B., 1985. The role of sulfate-reducing
9 bacteria in the deposition of sedimentary uranium ores. Geomicrobiology Journal
10 4, 153-173.
- 11 Mohanty, S.R., Kollah, B., Hedrick, D.B., Peacock, A.D., Kukkadapu, R.K., Roden, E.E.,
12 2008. Biogeochemical processes in ethanol stimulated uranium-contaminated
13 subsurface sediments. Environmental Science & Technology 42, 4384-4390.
- 14 Montgomery, D.M., Dean, A.C.R., Wiffen, P., Macaskie, L.E., 1995. Phosphatase
15 production and activity in citrobacter-freundii and a naturally-occurring, heavy-
16 metal-accumulating citrobacter sp. Microbiology-Uk 141, 2433-2441.
- 17 Moon, H.S., Komlos, J., Jaffe, P.R., 2007. Uranium reoxidation in previously bioreduced
18 sediment by dissolved oxygen and nitrate. Environmental Science & Technology
19 41, 4587-4592.
- 20 Murphy, Riley, 1962. A modified single solution method for determination of phosphate
21 in natural waters. Analytica Chimica Acta 26.

1 Murphy, W.M., Shock, E.L., 1999. Environmental aqueous geochemistry of actinides, in:
2 Burns, P.C.a.F., R. (Ed.), Uranium: Mineralogy, Geochemistry and the
3 Environment. Mineralogical Society of America, Washington, D.C.

4 NABIR, 2003. Bioremediation of Metals and Radionuclides, DOE.

5 North, N.N., Dollhopf, S.L., Petrie, L., Istok, J.D., Balkwill, D.L., Kostka, J.E., 2004.
6 Change in bacterial community structure during in situ Biostimulation of
7 subsurface sediment cocontaminated with uranium and nitrate. Applied and
8 Environmental Microbiology 70, 4911-4920.

9 Nriagu, J.O., 1972. Stability of vivianite and ion-pair formation in system $\text{Fe}_3(\text{PO}_4)_2$ -
10 H_3PO_4 - H_2O . Geochimica Et Cosmochimica Acta 36, 459-&.

11 Nyman, J.L., Marsh, T.L., Ginder-Vogel, M.A., Gentile, M., Fendorf, S., Criddle, C.,
12 2006. Heterogeneous response to biostimulation for U(VI) reduction in replicated
13 sediment microcosms. Biodegradation 17, 303-316.

14 Ohnuki, I., Kozai, N., Samadfam, M., Yasuda, R., Yamamoto, S., Narumi, K., Naramoto,
15 H., Murakami, T., 2004. The formation of autunite $(\text{Ca}(\text{UO}_2)_2(\text{PO}_4)_2 \cdot n\text{H}_2\text{O})$ within the leached layer of dissolving apatite: incorporation
16 mechanism of uranium by apatite. Chemical Geology 211, 1-14.

17 Payne, T.E., Davis, J.A., Waite, T.D., 1996. Uranium adsorption on ferrihydrite - Effects
18 of phosphate and humic acid. Radiochimica Acta 74, 239-243.

19 Petrie, L., North, N.N., Dollhopf, S.L., Balkwill, D.L., Kostka, J.E., 2003. Enumeration
20 and characterization of iron(III)-reducing microbial communities from acidic
21 subsurface sediments contaminated with uranium(VI). Applied and
22 Environmental Microbiology 69, 7467-7479.

23

1 Qatibi, A.I., Niviere, V., Garcia, J.L., 1991. *Desulfovibrio-alcoholovorans* sp. nov., a
2 sulfate-reducing bacterium able to grow on glycerol, 1,2-propanediol and 1,3-
3 propanediol. Archives of Microbiology 155, 143-148.

4 Rake, J.B., Eagon, R.G., 1980. Inhibition, but not uncoupling, of respiratory energy
5 coupling of 3 bacterial species by nitrite. Journal of Bacteriology 144, 975-982.

6 Regenspurg, S., Schild, D., Schafer, T., Huber, F., Malmstrom, M.E., 2009. Removal of
7 uranium(VI) from the aqueous phase by iron(II) minerals in presence of
8 bicarbonate. Applied Geochemistry 24, 1617-1625.

9 Roh, Y., Lee, S.R., Choi, S.K., Elless, M.P., Lee, S.Y., 2000. Physicochemical and
10 mineralogical characterization of uranium-contaminated soils. Soil & Sediment
11 Contamination 9, 463-486.

12 Rossolini, G.M., Schippa, S., Riccio, M.L., Berlutti, F., Macaskie, L.E., Thaller, M.C.,
13 1998. Bacterial nonspecific acid phosphohydrolases: physiology, evolution and
14 use as tools in microbial biotechnology. Cellular and Molecular Life Sciences 54,
15 833-850.

16 Sanford, R.A., Wu, Q., Sung, Y., Thomas, S.H., Amos, B.K., Prince, E.K., Loffler, F.E.,
17 2007. Hexavalent uranium supports growth of Anaeromyxobacter dehalogenans
18 and Geobacter spp. with lower than predicted biomass yields. Environmental
19 Microbiology 9, 2885-2893.

20 Schecher, W.D., McAvoy, D.C., 2001. MINEQL+: A Chemical Equilibrium Modeling
21 System, Version 4.5 for Windows, User's Manual. Research Software, Hallowell,
22 Maine.

1 Senko, J.M., Istok, J.D., Suflita, J.M., Krumholz, L.R., 2002. In-situ evidence for
2 uranium immobilization and remobilization. *Environmental Science &*
3 *Technology* 36, 1491-1496.

4 Senko, J.M., Mohamed, Y., Dewers, T.A., Krumholz, L.R., 2005a. Role for Fe(III)
5 minerals in nitrate-dependent microbial U(IV) oxidation. *Environmental Science*
6 *& Technology* 39, 2529-2536.

7 Senko, J.M., Suflita, J.M., Krumholz, L.R., 2005b. Geochemical controls on microbial
8 nitrate-dependent U(IV) oxidation. *Geomicrobiology Journal* 22, 371-378.

9 Sharp, J.O., Lezama-Pacheco, J.S., Schofield, E.J., Junier, P., Ulrich, K.-U., Chinni, S.,
10 Veeramani, H., Margot-Roquier, C., Webb, S.M., Tebo, B.M., Giammar, D.E.,
11 Bargar, J.R., Bernier-Latmani, R., 2011. Uranium speciation and stability after
12 reductive immobilization in aquifer sediments. *Geochimica Et Cosmochimica*
13 *Acta* 75, 6497-6510.

14 Shelobolina, E.S., Konishi, H., Xu, H.F., Roden, E.E., 2009. U(VI) Sequestration in
15 Hydroxyapatite Produced by Microbial Glycerol 3-Phosphate Metabolism.
16 *Applied and Environmental Microbiology* 75, 5773-5778.

17 Shelobolina, E.S., O'Neill, K., Finneran, K.T., Hayes, L.A., Lovley, D.R., 2003. Potential
18 for in situ bioremediation of a low-pH, high-nitrate uranium-contaminated
19 groundwater. *Soil & Sediment Contamination* 12, 865-884.

20 Sijbesma, W.F.H., Almeida, J.S., Reis, M.A.M., Santos, H., 1996. Uncoupling effect of
21 nitrite during denitrification by *Pseudomonas fluorescens*: An in vivo P-31-NMR
22 study. *Biotechnology and Bioengineering* 52, 176-182.

1 Singer, P.C., Stumm, W., 1970. Solubility of ferrous iron in carbonate-bearing waters.
2 Journal American Water Works Association 62, 198-&.

3 Sowder, A.G., Clark, S.B., Fjeld, R.A., 2001. The impact of mineralogy in the U(VI)-Ca-
4 PO₄ system on the environmental availability of uranium. Journal of
5 Radioanalytical and Nuclear Chemistry 248, 517-524.

6 Spain, A.M., Krumholz, L.R., 2011. Nitrate-Reducing Bacteria at the Nitrate and
7 Radionuclide Contaminated Oak Ridge Integrated Field Research Challenge Site:
8 A Review. Geomicrobiology Journal 28, 418-429.

9 Stewart, B.D., Mayes, M.A., Fendorf, S., 2010. Impact of Uranyl–Calcium–Carbonato
10 Complexes on Uranium(VI) Adsorption to Synthetic and Natural Sediments.
11 Environmental Science & Technology 44, 928-934.

12 Stookey, L.L., 1970. Ferrozine- A new spectrophotometric reagent for iron. Anal. Chem.
13 42, 779-&.

14 Stubbs, J.E., Elbert, D.C., Veblen, D.R., Zhu, C., 2006. Electron microbeam investigation
15 of uranium-contaminated soils from Oak Ridge, TN, USA. Environmental
16 Science & Technology 40, 2108-2113.

17 Stumm, W., Morgan, J.J., 1996. Aquatic chemistry : chemical equilibria and rates in
18 natural waters, 3rd ed. ed. Wiley, New York :.

19 Tessier, A., Campbell, P.G.C., Bisson, M., 1979. Sequential extraction procedure for the
20 speciation of particulate trace-metals. Anal. Chem. 51, 844-851.

21 Ulrich, K.U., Ilton, E.S., Veeramani, H., Sharp, J.O., Bernier-Latmani, R., Schofield,
22 E.J., Bargar, J.R., Giammar, D.E., 2009. Comparative dissolution kinetics of

1 biogenic and chemogenic uraninite under oxidizing conditions in the presence of
2 carbonate. *Geochimica Et Cosmochimica Acta* 73, 6065-6083.

3 Van Haverbeke, L., Vochten, R., Van Springel, K., 1996. Solubility and spectrochemical
4 characteristics of synthetic chernikovite and meta-ankoleite. *Mineralogical*
5 *Magazine* 60, 759-766.

6 Wade, R., DiChristina, T.J., 2000. Isolation of U(VI) reduction-deficient mutants of
7 *Shewanella putrefaciens*. *Fems Microbiology Letters* 184, 143-148.

8 Waite, T.D., Davis, J.A., Payne, T.E., Waychunas, G.A., Xu, N., 1994. Uranium(VI)
9 adsorption to ferrihydrite- application of a surface complexation model.
10 *Geochimica Et Cosmochimica Acta* 58, 5465-5478.

11 Wan, J.M., Tokunaga, T.K., Brodie, E., Wang, Z.M., Zheng, Z.P., Herman, D., Hazen,
12 T.C., Firestone, M.K., Sutton, S.R., 2005. Reoxidation of bio-reduced uranium
13 under reducing conditions. *Environmental Science & Technology* 39, 6162-6169.

14 Webb, S.M., 2005. SIXpack: a graphical user interface for XAS analysis using IFEFFIT.
15 *Physica Scripta T115*, 1011-1014.

16 Webb, S.M., Fuller, C.C., Tebo, B.M., Bargar, J.R., 2006. Determination of uranyl
17 incorporation into biogenic manganese oxides using X-ray absorption
18 spectroscopy and scattering. *Environmental Science & Technology* 40, 771-777.

19 Webb, S.M., Tebo, B.M., Bargar, J.R., 2005. Structural characterization of biogenic Mn
20 oxides produced in seawater by the marine bacillus sp strain SG-1. *American*
21 *Mineralogist* 90, 1342-1357.

22 Wellman, D.M., Gunderson, K.M., Icenhower, J.P., Forrester, S.W., 2007. Dissolution
23 kinetics of synthetic and natural meta-autunite minerals, X-3-n((n)+) (UO₂)(

1 PO₄) (2) center dot xH₂O, under acidic conditions. *Geochemistry Geophysics*
2 *Geosystems* 8.

3 Wellman, D.M., Icenhower, J.P., Owen, A.T., 2006. Comparative analysis of soluble
4 phosphate amendments for the remediation of heavy metal contaminants: Effect
5 on sediment hydraulic conductivity. *Environmental Chemistry* 3, 219-224.

6 Wersin, P., Hochella, M.F., Persson, P., Redden, G., Leckie, J.O., Harris, D.W., 1994.
7 Interaction between aqueous uranium(VI) and sulfide minerals - spectroscopic
8 evidence for sorption and reduction. *Geochimica Et Cosmochimica Acta* 58,
9 2829-2843.

10 Wielinga, B., Bostick, B., Hansel, C.M., Rosenzweig, R.F., Fendorf, S., 2000. Inhibition
11 of bacterially promoted uranium reduction: Ferric (hydr)oxides as competitive
12 electron acceptors. *Environmental Science & Technology* 34, 2190-2195.

13 Wu, W.M., Carley, J., Fienen, M., Mehlhorn, T., Lowe, K., Nyman, J., Luo, J., Gentile,
14 M.E., Rajan, R., Wagner, D., Hickey, R.F., Gu, B.H., Watson, D., Cirpka, O.A.,
15 Kitanidis, P.K., Jardine, P.M., Criddle, C.S., 2006a. Pilot-scale in situ
16 bioremediation of uranium in a highly contaminated aquifer. 1. Conditioning of a
17 treatment zone. *Environmental Science & Technology* 40, 3978-3985.

18 Wu, W.M., Carley, J., Gentry, T., Ginder-Vogel, M.A., Fienen, M., Mehlhorn, T., Yan,
19 H., Carroll, S., Pace, M.N., Nyman, J., Luo, J., Gentile, M.E., Fields, M.W.,
20 Hickey, R.F., Gu, B.H., Watson, D., Cirpka, O.A., Zhou, J.Z., Fendorf, S.,
21 Kitanidis, P.K., Jardine, P.M., Criddle, C.S., 2006b. Pilot-scale in situ
22 bioremediation of uranium in a highly contaminated aquifer. 2. Reduction of

1 U(VI) and geochemical control of U(VI) bioavailability. *Environmental Science*
2 & *Technology* 40, 3986-3995.

3 Wu, W.M., Carley, J., Green, S.J., Luo, J.A., Kelly, S.D., Van Nostrand, J., Lowe, K.,
4 Mehlhorn, T., Carroll, S., Boonchayanant, B., Lofler, F.E., Watson, D., Kemner,
5 K.M., Zhou, J.Z., Kitanidis, P.K., Kostka, J.E., Jardine, P.M., Criddle, C.S., 2010.
6 Effects of Nitrate on the Stability of Uranium in a Bioreduced Region of the
7 Subsurface. *Environmental Science & Technology* 44, 5104-5111.

8 Zabinsky, S.I., Rehr, J.J., Ankudinov, A., Albers, R.C., Eller, M.J., 1995. Multiple-
9 scattering calculations of X-ray absorption spectra. *Physical Review B* 52, 2995-
10 3009.

11 Zhang, F., Wu, W.-M., Parker, J.C., Mehlhorn, T., Kelly, S.D., Kemner, K.M., Zhang,
12 G., Schadt, C., Brooks, S.C., Criddle, C.S., Watson, D.B., Jardine, P.M., 2010.
13 Kinetic analysis and modeling of oleate and ethanol stimulated uranium (VI) bio-
14 reduction in contaminated sediments under sulfate reduction conditions. *Journal*
15 *of Hazardous Materials* 183, 482-489.

16 Zheng, Z.P., Tokunaga, T.K., Wan, J.M., 2003. Influence of calcium carbonate on U(VI)
17 sorption to soils. *Environmental Science & Technology* 37, 5603-5608.

18 Zheng, Z.P., Wan, J.M., Song, X.Y., Tokunaga, T.K., 2006. Sodium meta-autunite
19 colloids: Synthesis, characterization, and stability. *Colloids and Surfaces a-*
20 *Physicochemical and Engineering Aspects* 274, 48-55.

21
22
23

TABLES

Table 1. pH, U(VI), G2P, and external terminal electron acceptor (TEA) conditions in each incubation conducted in duplicate in artificial groundwater.

<i>Treatment</i>	<i>pH</i>	<i>[U(VI)]</i>	<i>[G2P]</i>	<i>[TEA]</i>
U - amended control	5.5/7.0	300 μ M	0 mM	0 mM
G2P - amended reactor	5.5/7.0	300 μ M	5.0 mM	0 mM
NO ₃ ⁻ - amended reactor	5.5	300 μ M	5.0 mM	7.0 mM NO ₃ ⁻
NO ₃ ⁻ - amended reactor	7.0	300 μ M	0 mM	7.0 mM NO ₃ ⁻
SO ₄ ²⁻ - amended reactor	5.5/7.0	300 μ M	5.0 mM	9.4 mM SO ₄ ²⁻

Table 2. Pseudo-first-order rate constants, k_{obs} , for consumption of NO₃⁻, Fe(III), glycerol-2-phosphate (G2P), and dissolved U. For pH 7.0 reactors, only one uranium rate constant was calculated between days 0 and 30. Rate constants reported as N/A represent species that were not present in the given reactor treatment, and rate constants reported as 0 represent species that were not transformed between the initial and final sampling points. Values are reported in units of d⁻¹. Errors represent the standard error of the unweighted slope of linear regressions used to determine rate constants (details in supplementary material).

<i>Treatment</i>	<i>pH</i>	<i>NO₃⁻</i>	<i>Fe(III)</i>	<i>G2P</i>	<i>U</i>
U - amended control	5.5	0	0.66 \pm 0.01	N/A	0
	7.0	0	1.36 \pm 0.03	N/A	0
G2P - amended reactor	5.5	0.04 \pm 0.01	0.62 \pm 0.02	0.05 \pm 0.01	0.39 \pm 0.01 ^a 0.10 \pm 0.01 ^b
	7.0	0.07 \pm 0.03	1.28 \pm 0.01	0.10 \pm 0.00	0.06 \pm 0.01
SO ₄ ²⁻ - amended reactor	5.5	0.04 \pm 0.01	0.64 \pm 0.01	0.05 \pm 0.01	0.39 \pm 0.09 ^a 0.11 \pm 0.02 ^b
	7.0	0.06 \pm 0.01	1.38 \pm 0.04	0.09 \pm 0.02	0.06 \pm 0.01
NO ₃ ⁻ - amended reactor	5.5	0.02 \pm 0.00	0.54 \pm 0.01	0.05 \pm 0.02	0.46 \pm 0.08 ^a 0.10 \pm 0.01 ^b
	7.0	0	1.36 \pm 0.02	N/A	0

^a Calculated rate constant between day 0 and day 4 representing the initial uranium removal phase

^b Calculated rate constant between day 7 and day 31 representing the secondary removal phase

Table 3. Fitting Parameters for U L_{III}-edge EXAFS derived using SIXPACK (Webb, 2005) in pH 5.5 reactors. Treatments include a (300 μ M U, day 70), b (300 μ M U + 5 mM G2P, day 0), c (300 μ M U + 5 mM G2P, day 70), d (300 μ M U + 5 mM G2P + 7 mM NO₃⁻, day 70), and e (300 μ M U + 5 mM G2P + 9.4 mM SO₄³⁻, day 70). *N* represents U-ligand coordination number, *R*(Å) represents U-ligand distance.

<i>Path</i>	<i>Treatment</i>	<i>N</i>	<i>R</i> (Å)	σ^2	<i>Rfactor</i>	ΔE_0
U-O _{ax}	a	2.00	1.80 ± 0.01	0.002 ± 0.001	0.0556	11.4 ± 2.92
	b	2.00	1.79 ± 0.01	0.001 ± 0.000	0.0399	9.63 ± 2.01
	c	2.00	1.80 ± 0.01	0.002 ± 0.001	0.0367	9.99 ± 2.29
	d	2.00	1.79 ± 0.01	0.002 ± 0.001	0.0522	8.22 ± 2.87
	e	2.00	1.76 ± 0.01	0.002 ± 0.001	0.0345	2.82 ± 3.07
U-O _{eq 2.30}	a	2.34 ± 0.65	2.30 ± 0.03	0.003		
	b	3.49 ± 0.55	2.35 ± 0.01	0.003		
	c	3.01 ± 0.55	2.34 ± 0.02	0.003		
	d	3.14 ± 0.63	2.30 ± 0.02	0.003		
	e	2.94 ± 0.58	2.22 ± 0.02	0.003		
U-O _{eq 2.45}	a	2.60 ± 0.75	2.46 ± 0.03	0.003		
	b	2.14 ± 0.71	2.53 ± 0.02	0.003		
	c	1.86 ± 0.70	2.52 ± 0.03	0.003		
	d	2.33 ± 0.76	2.47 ± 0.03	0.003		
	e	3.44 ± 0.62	2.39 ± 0.02	0.003		
U-Mn/Fe	a	0.20 ± 0.39	3.54 ± 0.01	0.003		
	b	0.32 ± 0.29	3.29 ± 0.05	0.003		
	c	0.36 ± 0.54	3.41 ± 0.06	0.003		
	d	0.31 ± 1.99	3.52 ± 0.27	0.003		
	e	0.40 ± 0.28	3.28 ± 0.04	0.003		
U-P	a					
	b					
	c	0.17 ± 1.11	3.62 ± 0.33	0.003		
	d	0.57 ± 2.32	3.60 ± 0.40	0.003		
	e	0.75 ± 0.71	3.72 ± 0.06	0.003		

Errors are given for values which were allowed to float
No error means value was fixed or calculated from other parameters

Table 4. Fitting Parameters for U L_{III}-edge EXAFS derived using SIXPACK (Webb, 2005) in pH 7.0 reactors. Treatments include a (300 μ M U, day 70), b (300 μ M U + 7 mM NO₃⁻, day 70), c (300 μ M U + 5 mM G2P, day 70), and d (300 μ M U + 5 mM G2P + 9.4 mM SO₄³⁻, day 70). *N* represents U-ligand coordination number, *R*(\AA) represents U-ligand distance.

<i>Path</i>	<i>Treatment</i>	<i>N</i>	<i>R</i> (\AA)	σ^2	<i>Rfactor</i>	ΔE_0
U-O _{ax}	a	2.00	1.87 \pm 0.01	0.008 \pm 0.002	0.0252	13.9 \pm 3.1
	b	2.00	1.86 \pm 0.04	0.006 \pm 0.003	0.0436	10.4 \pm 3.6
	c	2.00	1.85 \pm 0.03	0.005 \pm 0.003	0.0555	7.45 \pm 3.9
	d	2.00	1.78 \pm 0.01	0.007 \pm 0.001	0.0128	2.34 \pm 1.4
U-O _{eq 2.30}	a	1.37 \pm 0.49	2.30 \pm 0.03	0.003		
	b	1.35 \pm 1.6	2.28 \pm 0.10	0.003		
	c	2.05 \pm 2.5	2.25 \pm 0.06	0.003		
	d	1.72 \pm 0.31	2.20 \pm 0.02	0.003		
U-O _{eq 2.45}	a	1.64 \pm 0.58	2.46 \pm 0.02	0.003		
	b	2.65 \pm 2.19	2.44 \pm 0.07	0.003		
	c	3.73 \pm 3.22	2.42 \pm 0.04	0.003		
	d	1.96 \pm 0.37	2.35 \pm 0.02	0.003		
U-C	a					
	b	1.19 \pm 1.39	2.87 \pm 0.06	0.003		
	c					
	d	1.67 \pm 0.62	2.95 \pm 0.03	0.003		
U-Mn/Fe	a	0.27 \pm 0.14	3.43 \pm 0.03	0.003		
	b	0.49 \pm 0.42	3.47 \pm 0.06	0.003		
	c	0.30 \pm 0.43	3.18 \pm 0.07	0.003		
	d	0.43 \pm 0.16	3.24 \pm 0.02	0.003		
U-P	a					
	b					
	c	1.02 \pm 1.14	3.61 \pm 0.06	0.003		
	d	0.62 \pm 0.35	3.69 \pm 0.03	0.003		
Errors are given for values which were allowed to float						
No error means value was fixed or calculated from other parameters						

Table 5. Predicted solution equilibrium and solid phase saturation indices using MINEQL+ (Schecher and McAvoy, 2001) in pH 5.5 and 7.0 incubations assuming 5 mM ΣPO_4^{3-} was produced by G2P hydrolysis. Solution concentrations are reported in percent of total species. Each treatment (Table 1) was modeled using the maximum measured total Fe^{2+} concentration and initial conditions as input for all other species. A double layer sorption model onto amorphous Fe-oxide (3.2 g/L, 600 m²/g surface area) was included in the calculations. Unless otherwise noted, log K values are as reported in Schecher and McAvoy (2001).

Species	Log K	Treatment			
		U - amended control	G2P - amended reactor	SO ₄ ²⁻ - amended reactor	NO ₃ ⁻ - amended reactor
pH 5.5					
UO ₂ ²⁺					
UO ₂ CO ₃ (aq)	9.94 ^a	25.9%	0.1%	0.0%	0.1%
Fe(wk)OH-UO ₂ (OH) ₂	-6.28 ^b		0.0%	0.0%	0.0%
Fe(st)OH-UO ₂ (OH) ₂	-2.57 ^b		0.7%	0.3%	0.4%
Others	--	6.8%	--	--	--
PO ₄ ³⁻					
Fe(wk)H ₂ PO ₄	31.29	--	44.7%	48.4%	48.4%
Fe(wk)HPO ₄ ⁻	25.39	--	45.5%	41.6%	41.6%
Others (Autunite)	--	--	9.9%	10.0%	10.0%
Fe ²⁺					
Fe ²⁺		91.3%	93.4%	57.5%	94.7%
Fe(st)OH-Fe(OH) ⁺	-0.95 ^c	0.0%	3.60%	2.70%	2.80%
Fe(wk)-Fe(OH) ⁺	-2.98 ^c	6.8%	1.50%	1.10%	1.10%
Others	--	1.9%	1.5%	1.5%	1.4%
Solid Phase					
Schoepite	-5.2 ^d	-0.981	-3.48	-3.84	-3.70
Na-Autunite	47.4	-28.4	0 (99.2% U)	0 (99.7% U)	0 (99.5% U)
Ca-Autunite	44.7 ^d	-32.05	-3.51	-4.16	-3.88
K-Autunite	22.73 ^e	-28.64	-0.19	-0.72	-0.44
Vivianite	36.0 ^f	-40.62	-7.10	-6.99	-6.98
Siderite	10.24 ^g	-3.24	-3.20	-3.25	-3.24
pH 7.0					
UO ₂ ²⁺					
UO ₂ (CO ₃) ₂ ⁻²	16.61 ^a	11.3%	0.1%	0.1%	12.3%
CaUO ₂ (CO ₃) ₃ ⁻²	27.18 ^h	28.4%	0.5%	0.2%	27.8%
Ca ₂ UO ₂ (CO ₃) ₃ ⁰	30.7 ^h	6.4%	0.2%	0.1%	6.0%
Fe(st)OH-UO ₂ (OH) ₂	-2.57 ^b	47.3%	0.0%	0.0%	47.3%
Others	--	6.6%	--	--	6.6%
PO ₄ ³⁻					
Fe(wk)H ₂ PO ₄	31.29	--	23.7%	22.8%	--
Fe(wk)HPO ₄ ⁻	25.39	--	61.9%	62.6%	--
Others	--	--	14.4%	14.6%	--
Fe ²⁺					
Fe ²⁺		4.4%	38.2%	34.8%	4.5%
Fe(wk)-Fe(OH) ⁺	-2.98 ^c	71.3%	47.8%	40.5%	71.1%
Fe(st)OH-Fe(OH) ⁺	-0.95 ^c	22.3%	7.00%	8.60%	22.4%
Fe(wk)-Fe(OH) ₂	-11.55 ^c	1.9%	1.30%	1.10%	1.9%
Others	--	0.1%	5.7%	15.0%	0.1%
Solid Phase					
Schoepite	-5.2 ^d	-2.32	-4.30	-4.50	-2.32
Na-Autunite	47.4	-32.21	0 (99.2% U)	0 (99.6% U)	-32.00
Ca-Autunite	44.7 ^d	-35.95	-3.65	-4.29	-35.98
K-Autunite	22.73 ^e	-32.42	-0.19	-0.72	-32.45
Vivianite	36.0 ^f	-39.70	-0.63	-0.97	-39.72
Siderite	10.24 ^g	-2.35	-1.34	-1.44	-2.36

^a (Guillaumont et al., 2003), ^b (Waite et al., 1994), ^c (Appelo et al., 2002), ^d (Langmuir, 1997), ^e (Van Haverbeke et al., 1996), ^f (Nriagu, 1972), ^g (Singer and Stumm, 1970), ^h (Dong and Brooks, 2006)

FIGURE CAPTIONS

Figure 1: Evolution of SO_4^{2-} [(A) and (B)], NO_3^- and NO_2^- [(C) and (D)], $\text{Fe}^{2+}_{(\text{aq})}$ and adsorbed Fe^{2+} [(E) and (F)], and Glycerol-2-phosphate (G2P) and $\sum\text{PO}_4^{3-}$ [(G) and (H)] as a function of time in pH 5.5 [(A), (C), (E), and (G)] and pH 7.0 [(B), (D), (F), and (H)] static microcosms amended with 300 μM UO_2^{2+} only; 300 μM UO_2^{2+} and 7 mM NO_3^- (pH 7.0 only); 300 μM UO_2^{2+} and 5 mM G2P; 300 μM UO_2^{2+} , 5 mM G2P, and 7 mM NO_3^- (pH 5.5 only); or 300 μM UO_2^{2+} , 5 mM G2P, and 9.4 mM SO_4^{2-} . Grey symbols represent chemical species on the left axes, while black symbols represent chemical species on the right axes. Error bars represent the range of average reported concentrations between duplicate reactors.

Figure 2: Evolution of A) Total dissolved uranium as a function of time in pH 5.5 (open symbols) and pH 7.0 (closed symbols) static microcosms amended with 300 μM UO_2^{2+} only; 300 μM UO_2^{2+} and 7 mM NO_3^- (pH 7.0 only); 300 μM UO_2^{2+} and 5 mM G2P; 300 μM UO_2^{2+} , 5 mM G2P, and 7 mM NO_3^- (pH 5.5 only); or 300 μM UO_2^{2+} , 5 mM G2P, and 9.4 mM SO_4^{2-} . Error bars represent the range of average reported values between duplicate reactors, and uranium standard deviations also include error associated with duplicate measurements. B) Linearization of total dissolved uranium in all reactors assuming pseudo-first-order with respect to uranium concentration. For pH 5.5 reactors, data points between 0 and 4 days have a distinct linear fit from data points between 7 and 39 days.

1 **Figure 3:** Solid phase-associated ΣPO_4^{3-} extracted with uranium by the sequential
2 extraction technique of Tessier (1979) from **A)** pH 5.5 and **B)** pH 7.0 sediments after 70
3 days of incubation. Bars represent the species extracted during each individual extraction
4 step. A total of $4.4 (\pm 0.7) \mu\text{mol g}^{-1}$ soil ΣPO_4^{3-} was extracted from the untreated soils.
5 All error bars represent the standard error of the mean calculated from duplicate reactors
6 and duplicate extractions.

7
8 **Figure 4:** Solid phase-associated U extracted by the sequential extraction technique of
9 Tessier (1979) from **A)** pH 5.5 and **B)** pH 7.0 sediments after 70 days of incubation. A
10 total of $0.7 (\pm 0) \mu\text{mol g}^{-1}$ soil U was extracted from the untreated soils. Bars represent
11 percent uranium extracted in each individual extraction step with respect to the total
12 extracted uranium in each treatment. Symbols represent the percent uranium recovered
13 in each reactor with respect to the total mass of extractable uranium. All error bars
14 represent the standard error of the mean calculated from duplicate reactors and duplicate
15 extractions.

16
17 **Figure 5:** Uranium (A) XANES, (B) R-space, and (C) *k*-space diagrams of the L_{III} -edge
18 EXAFS obtained from Area 3 sediments of the Oak Ridge Field Research Center
19 incubated anaerobically in static microcosms for 70 days at pH 5.5. Treatments included
20 a (300 μM U + 5 mM G2P, day 0), b (300 μM U + 5 mM G2P, day 70), c (300 μM U + 5
21 mM G2P + 7 mM NO_3^- , day 70), d (300 μM U + 5 mM G2P + 9.4 mM SO_4^{3-} , day 70),
22 and e (300 μM U, day 70).

1 **Figure 6:** Uranium (A) XANES, (B) R-space, and (C) *k*-space diagrams of the L_{III}-edge
2 EXAFS obtained from Area 3 sediments of the Oak Ridge Field Research Center
3 incubated anaerobically in static microcosms for 70 days at pH 7.0. Treatments included
4 a (300 μM U, T = 70 d), b (300 μM U + 7 mM NO₃⁻, T = 70 d), c (300 μM U + 5 mM
5 G2P, T = 70 d), and d (300 μM U + 5 mM G2P + 9.4 mM SO₄³⁻, T = 70 d).
6

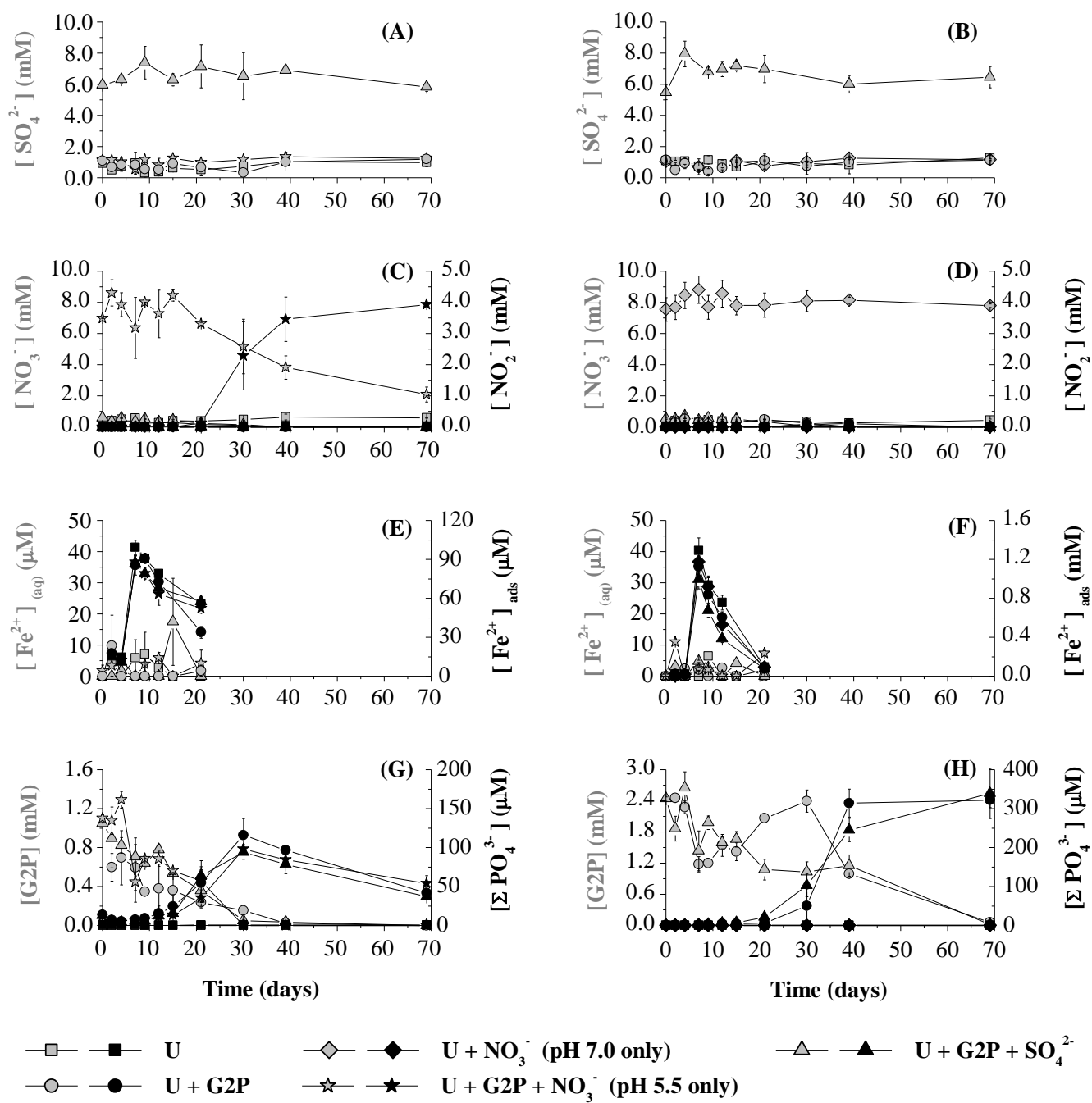


Figure 1. – Salome et al., 2012

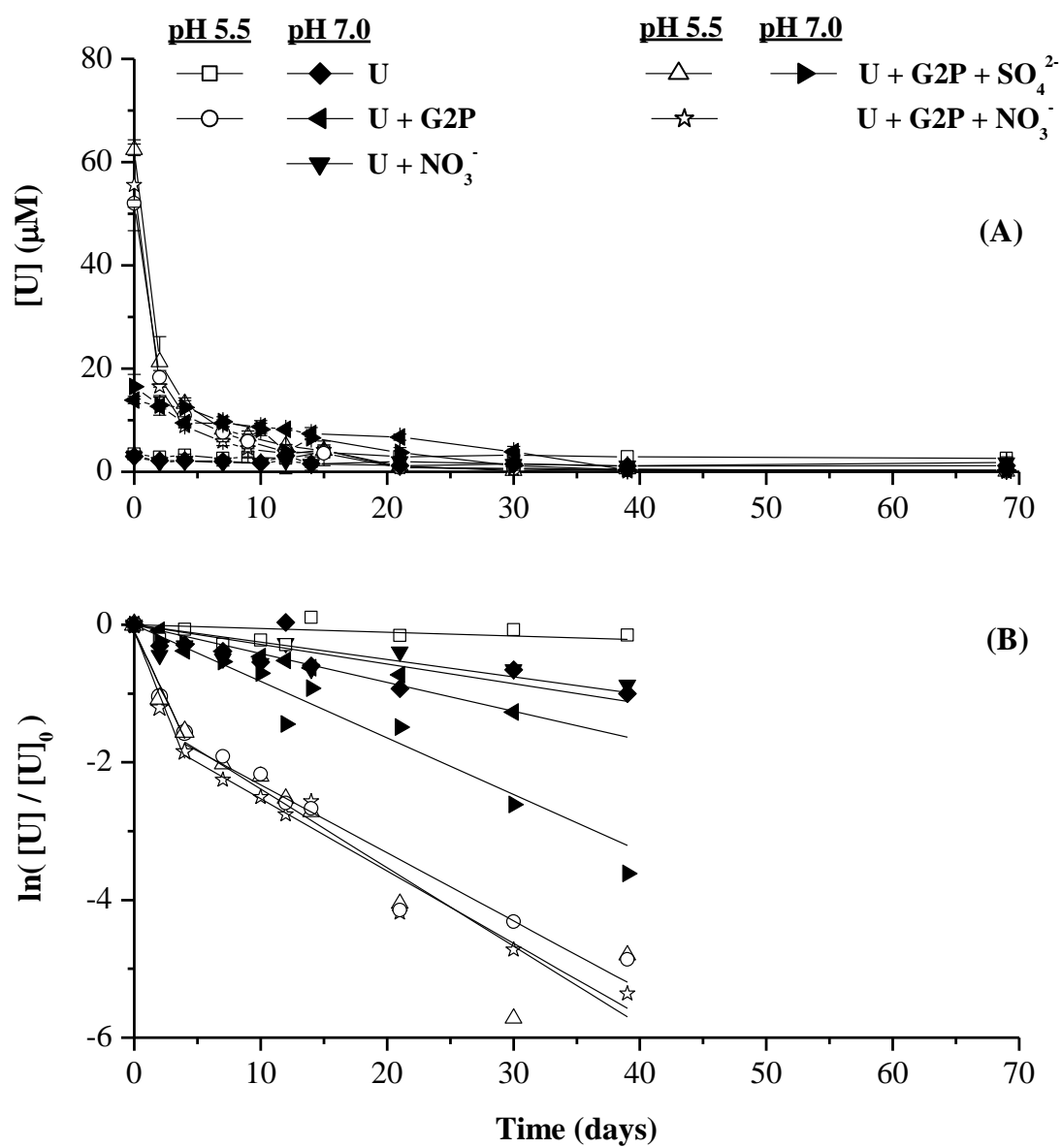


Figure 2. – Salome et al., 2012

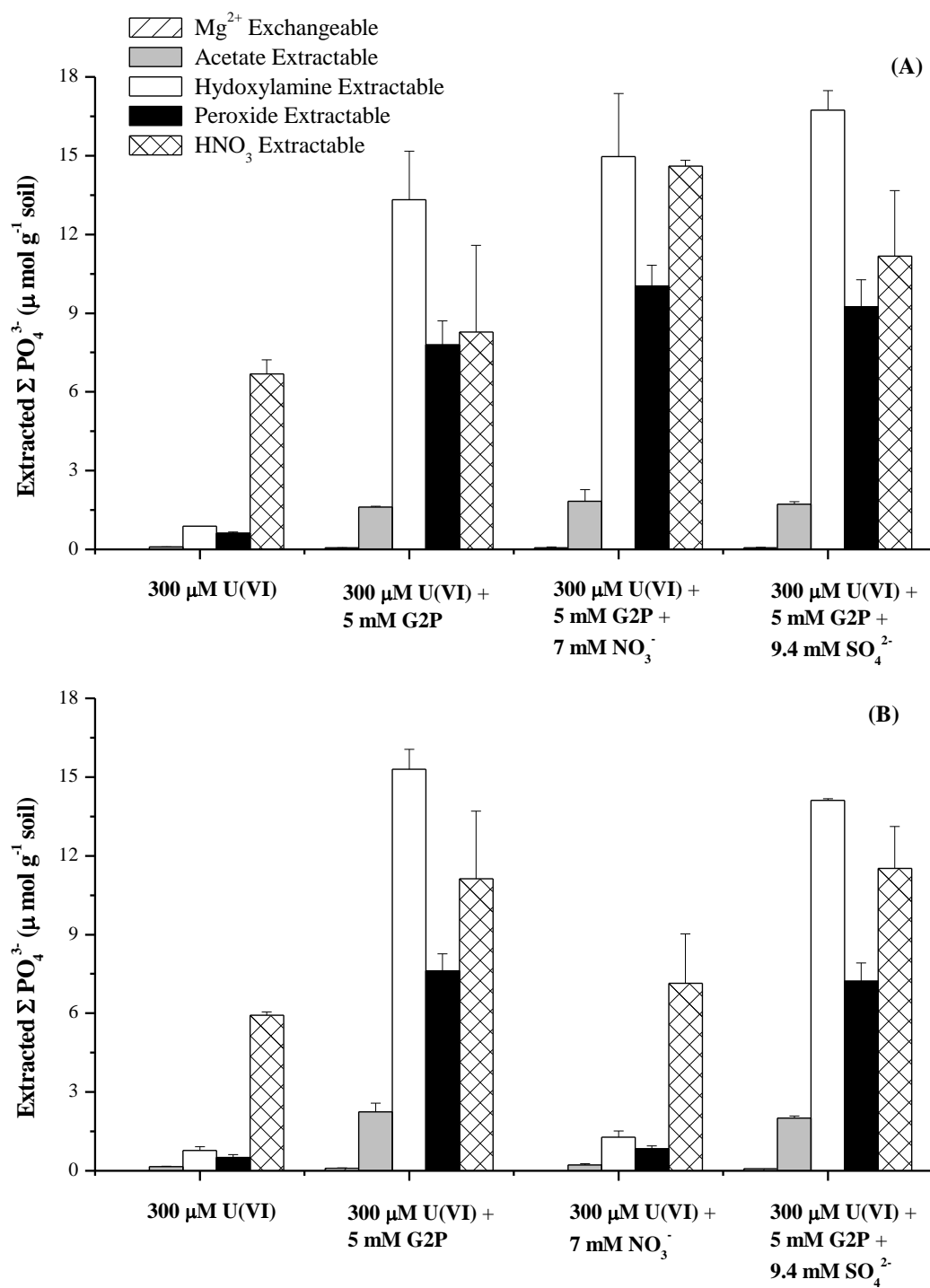


Figure 3- Salome et al., 2012

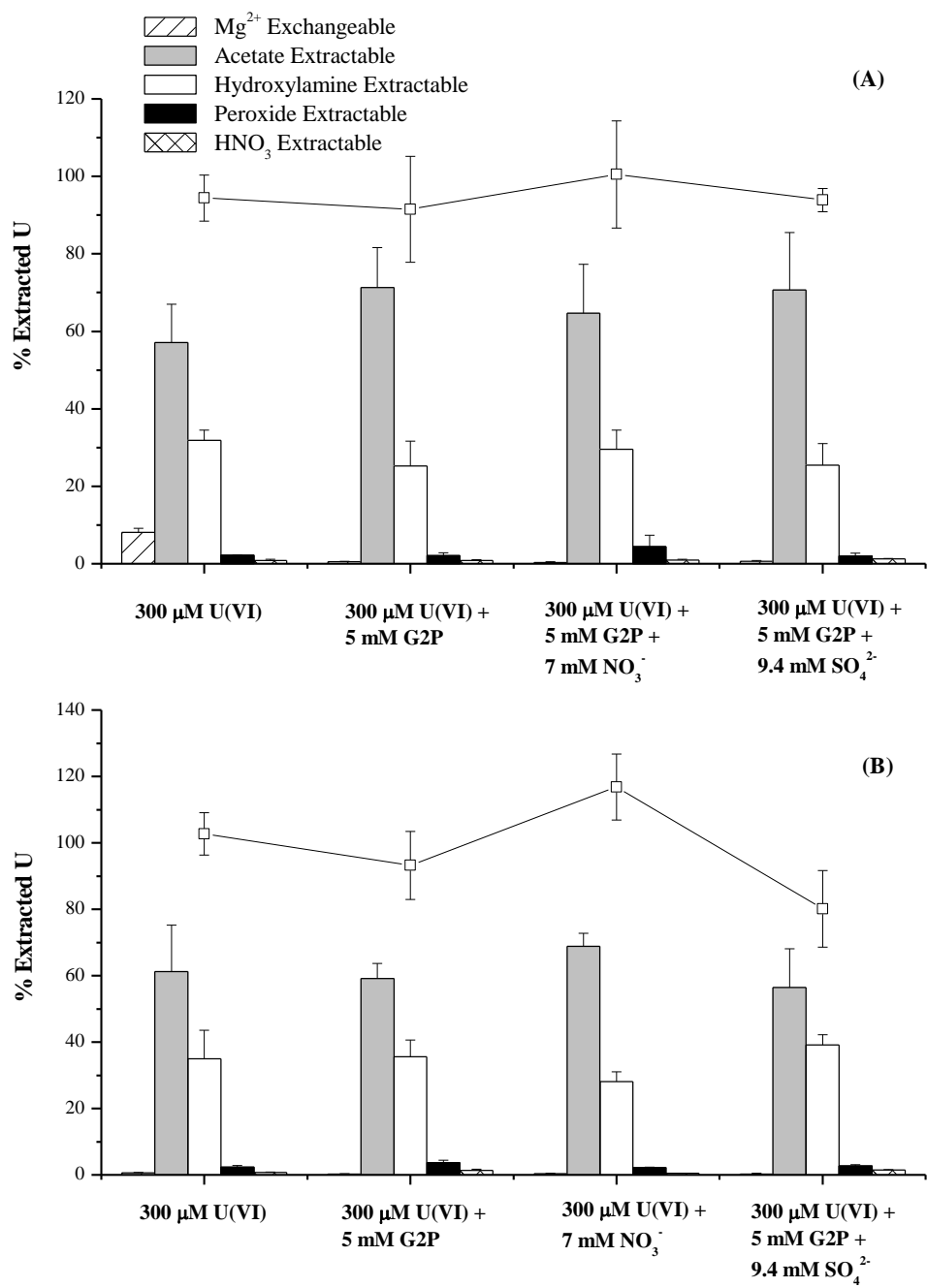


Figure 4- Salome et al., 2012

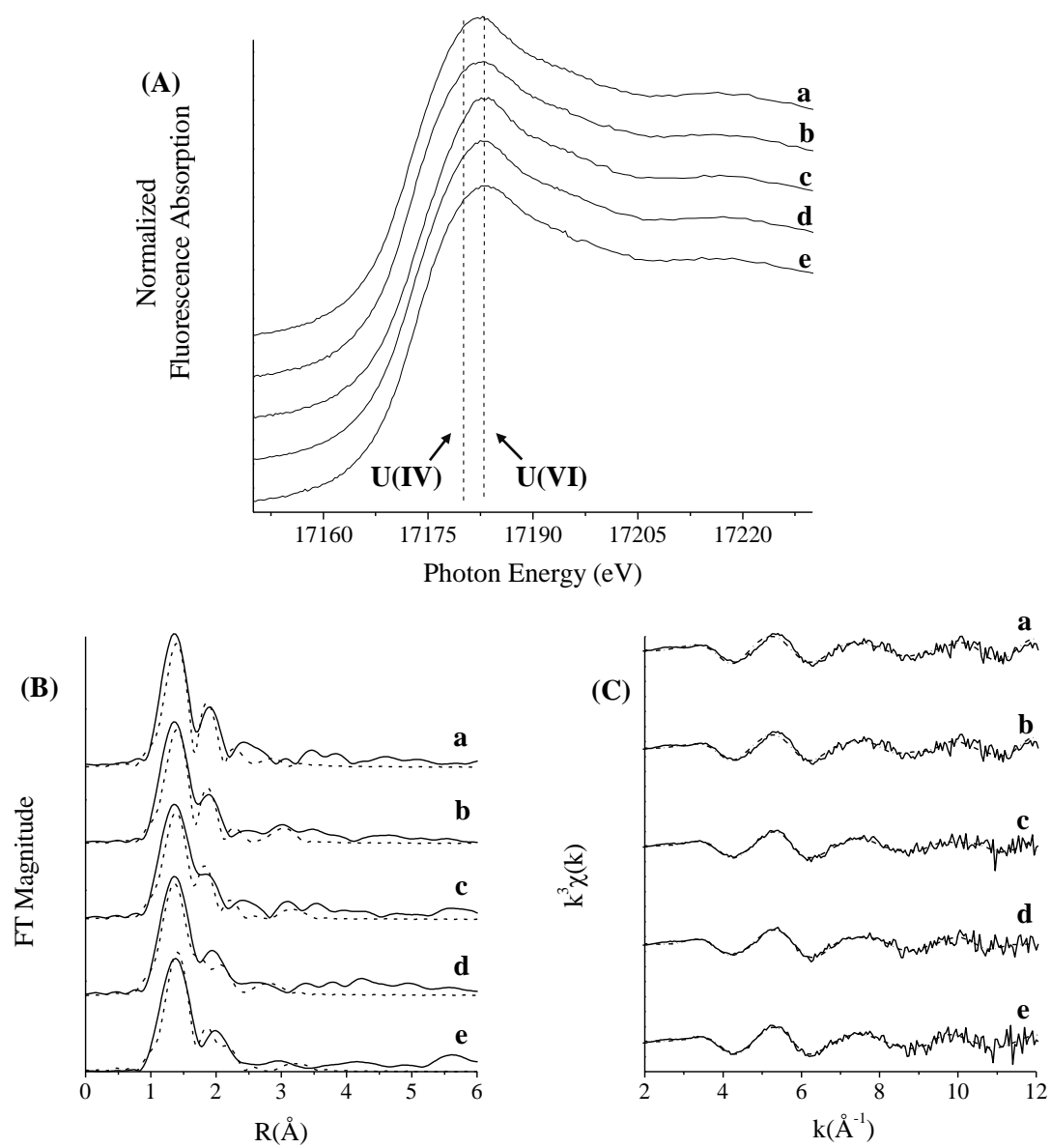


Figure 5- Salome et al., 2012

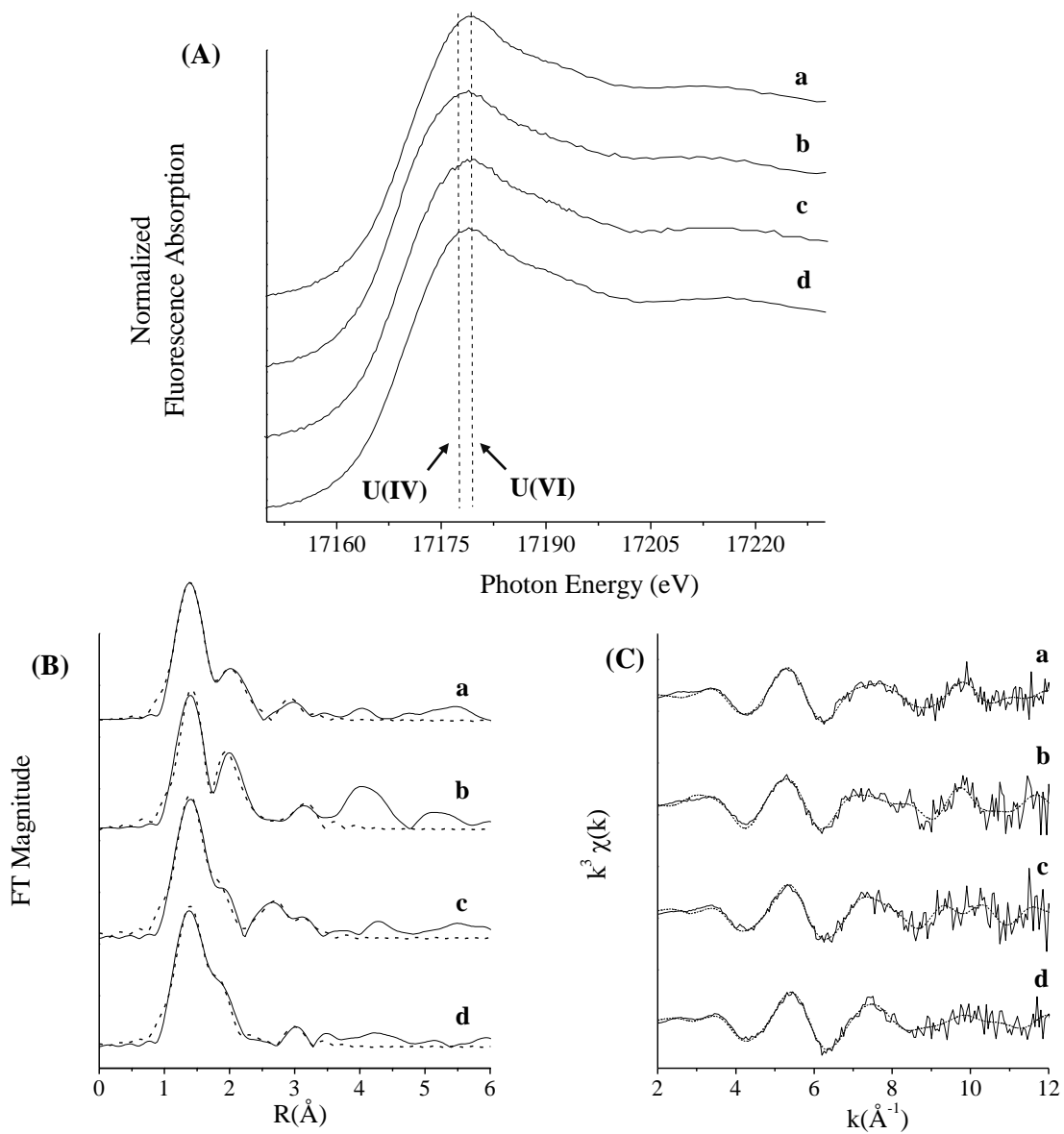


Figure 6- Salome et al., 2012